

TOPICAL REVIEW

Precursor films in wetting phenomena

M N Popescu^{1,2}, G Oshanin³, S Dietrich^{2,4}, and A-M Cazabat⁵¹ Ian Wark Research Institute, University of South Australia, Adelaide, SA 5095, Australia² Max Planck Institute for Intelligent Systems, Heisenbergstr. 3, 70569 Stuttgart, Germany³ Laboratoire de Physique Théorique de la Matière Condensée (UMR CNRS 7600), Université Pierre et Marie Curie, 4 place Jussieu F-75252, Paris Cedex 05, France⁴ Institut für Theoretische und Angewandte Physik, Universität Stuttgart, Pfaffenwaldring 57, 70569 Stuttgart, Germany⁵ Laboratoire de Physique Statistique (UMR CNRS 8550), Université Pierre et Marie Curie and Ecole Normale Supérieure, 24 rue Lhomond 75231 Paris Cedex 05, France

E-mail: Mihail.Popescu@unisa.edu.au, oshanin@lptmc.jussieu.fr, dietrich@is.mpg.de, anne-marie.cazabat@upmc.fr

Abstract. The spontaneous spreading of non-volatile liquid droplets on solid substrates poses a classic problem in the context of wetting phenomena. It is well known that the spreading of a macroscopic droplet is in many cases accompanied by a thin film of macroscopic lateral extent, the so-called precursor film, which emanates from the three-phase contact line region and spreads ahead of the latter with a much higher speed. Such films have been usually associated with liquid-on-solid systems, but in the last decade similar films have been reported to occur in solid-on-solid systems. While the situations in which the thickness of such films is of mesoscopic size are rather well understood, an intriguing and yet to be fully understood aspect is the spreading of microscopic, i.e., molecularly thin films. Here we review the available experimental observations of such films in various liquid-on-solid and solid-on-solid systems, as well as the corresponding theoretical models and studies aimed at understanding their formation and spreading dynamics. Recent developments and perspectives for future research are discussed.

PACS numbers: 47.55.nd, 68.08.Bc

Contents

1	Introduction	2
2	Droplets on solid substrates: equilibrium versus non-equilibrium	4
2.1	Partial wetting	4
2.1.1	Thermodynamic equilibrium.	4
2.1.2	Non-equilibrium behaviour.	6
2.2	Complete wetting	6

3	Spreading of non-volatile droplets	6
3.1	Non-volatile droplet spreading at macroscopic scales	7
3.2	Non-volatile droplet spreading at mesoscopic scales: mesoscopic films .	9
3.2.1	Experimental evidence.	9
3.2.2	Theoretical concepts.	10
3.3	Non-volatile droplet spreading at microscopic scales: ultrathin molecular films	13
4	Experimental studies of spreading of microscopic precursor films	13
4.1	Molecularly thin precursor films in liquid-on-solid systems	13
4.2	Ultrathin precursor films in metal-on-metal systems	21
5	Models for the dynamics of spreading of microscopic precursors	25
6	Numerical studies of ultrathin precursors	31
6.1	Monte Carlo simulations	31
6.2	Molecular Dynamics simulations for simple or polymeric liquids . . .	33
6.3	Molecular Dynamics simulations for metal-on-metal systems	39
7	Recent developments	42
8	Summary and outlook	43
	Acknowledgements	44
	References	44

1. Introduction

Wetting of a solid by a liquid is a very common natural phenomenon. Morning dew on the grass, rain drops on the plant leaves or windows, the coffee spill staining the table cloth, the water rise in the capillaries of a tree, the lubricating film covering the eye, or the oil drops on a non-sticky frying pan are examples of wetting in day-to-day life. As much as being a ubiquitous natural phenomenon, wetting is at the core of many technologies and technological processes vital for various industries [1–3], e.g., the protective spin coating of surfaces (CDs, DVDs, glass lenses, car mirrors and windows), the development of water-resistant fabric, ink-jet printing, wall-painting, froth flotation [4] or acid heap leaching [5] in minerals recovery.

The theoretical analysis of wetting phenomena has been started more than two hundred years ago by Young [6], Laplace [7] and Plateau [8]. Their descriptions and the related subsequent developments are usually referred to as classical capillarity. Based on the seminal work by Gibbs [9], the theory of molecular liquids in terms of statistical physics led to a good (and still progressing) understanding of their bulk equilibrium properties [10, 11]. The theoretical description of the structure and properties of free liquid-vapor interfaces [12–15], as well as of the equilibrium wetting transitions occurring at an inert wall exposed to a fluid which is in a thermodynamic state close to bulk liquid-vapor coexistence, have also reached a mature state [16–19]. (For rather recent developments see Refs. [20–23] and references therein.) †

† Unfortunately size constraints make it impossible to do justice to all the numerous important

These contributions have put forward a thermodynamic and mechanical description of capillarity which is successful in explaining a large number of phenomena such as capillary rise, the shape of sessile or pendant drops and the shape of a meniscus, at least as long as only macroscopic phenomena are involved. The physico-chemical parameters controlling the thermodynamic wettability of solid surfaces were clarified through the careful work of Zisman [24] and colleagues (see, e.g., Ref. [1]).

In the last two decades, significant efforts have been made towards understanding wetting phenomena at mesoscopic and microscopic scales. This was facilitated by the development of modern experimental techniques, capable of probing interfacial structures down to molecular scales, together with the fast paced technological progress in the fabrication of patterned surfaces possessing lateral wetting properties tailored on the micron- or even nano-scale through surface chemistry or topography. In this review, we focus solely on one particular subject in this area, i.e., the spreading of molecularly thin precursor films emanating from droplets deposited on solid substrates.

Since the late 1980s much progress has been achieved, both experimentally and theoretically, towards the understanding of the spreading dynamics of such films. Not only their occurrence in various liquid-on-solid systems has been reported in numerous studies, but also various details about their spatio-temporal structure have been revealed. Moreover, molecularly thin precursor films have been discovered in metal-on-metal systems, including even the case of films emerging out of solid clusters. The rich behaviour observed in these latter systems, which includes surface alloying, is at present a topic of active investigations. The rapidly developing nano-fluidics chip technology keeps the interest in such films high by raising new questions, such as the spreading behaviour of sub-micron scale drops or their motion induced by such precursor films [25]. On the theoretical side, a number of models have been proposed in order to explain the experimentally observed behaviour.

However, these results are scattered in the literature and up to date no attempt has been made to present a comprehensive review. In particular Ref. [26], which dates back to 1991, covered only the few results concerning the dynamics of microscopic precursor films available during the short period since 1989, when the first reports on this topic appeared [27–30]. The recent review of dynamics of wetting in Ref. [31] has only briefly touched this subject because it was not within its main scope. Here we strive for overcoming this dearth by collecting and assessing the large body of available experimental results, both for liquid-on-solid and solid-on-solid systems, and by discussing the various attempts of theoretical and numerical modeling the spreading of microscopically thin precursor films.

This review is outlined as follows. In Section 2 we briefly recall certain general thermodynamic criteria for the thermodynamic equilibrium of a macroscopic (but sufficiently small for the capillary forces dominating external ones, such as gravity) liquid drop on a solid substrate. In Section 3 we focus on spontaneous spreading of a droplet. In order to put the subject into a broader context (and in order to avoid referring an interested reader to the seminal original papers too often), there we concisely discuss the characteristic features of the spreading of the macroscopic part of the droplet, the emergence of a mesoscopic precursor film, and its dynamics. Size constraints do not permit to provide a more detailed discussion of all seminal contributions. An interested reader can find such a description in comprehensive

contributions to the understanding of equilibrium wetting phenomena. The interested reader is encouraged to consult the extended bibliography lists in, e.g., Refs. [13, 16, 18].

reviews [16, 26, 31]. Next, in Section 4 we turn to the subject of interest here and we overview experimental data on spreading of microscopically thin precursor films in different liquid-on-solid and solid-on-solid systems. Section 5 presents various theoretical models of microscopic precursor films, while Section 6 focuses on numerical simulations of these systems. Section 7 presents the recent developments in this area. Finally, in Section 8 we provide a summary and an outlook.

2. Droplets on solid substrates: equilibrium versus non-equilibrium

One of the often encountered realizations of wetting is that of a liquid drop on a planar solid substrate. For this setup, two limiting cases are well-defined: (i) a thermodynamic equilibrium situation [‡] with a liquid droplet on a solid substrate and the latter covered by a thin film, both in contact with the saturated coexisting vapour phase in a bounded system, and (ii) a non-equilibrium situation with late-stage spreading (so that all transient effects, e.g., the ones due to the initial shape, have died out) of a droplet of a non-volatile liquid on an otherwise “dry” solid substrate.

2.1. Partial wetting

2.1.1. Thermodynamic equilibrium. In the thermodynamic equilibrium situation, three distinct interfaces meet at a contact line [see Fig. 1(a)]: the liquid-vapour, the liquid-solid and the solid-vapour interfaces with the corresponding well-defined surface tensions σ_{lv} , σ_{ls} , and σ_{sv} , respectively. Note that σ_{sv} takes into account the presence of a thin liquid-like wetting film intervening between the solid substrate and the vapour phase [18]. In the case of a macroscopically large drop (but with a linear size smaller than the capillary length $\chi = \sqrt{\sigma_{lv}/(\rho g)}$, where ρ is the mass density of the liquid and g the gravitational constant) on a perfectly smooth, chemically homogeneous, and planar substrate (to which we shall constrain most of our discussion) the equilibrium contact angle θ_∞ [see Fig. 1(a)] is determined by Young’s equation

$$\sigma_{lv} \cos \theta_\infty = \sigma_{sv} - \sigma_{sl}. \quad (1)$$

Note that θ_∞ is understood to be measured macroscopically, on a scale large compared with the range of long-ranged intermolecular forces. In terms of the so-called spreading coefficient (also often called the spreading “power”)

$$S = \sigma_{sv} - \sigma_{lv} - \sigma_{sl}, \quad (2)$$

one can rewrite Eq. (1) as

$$\cos \theta_\infty = 1 + \frac{S}{\sigma_{lv}}, \quad (3)$$

which relates the equilibrium contact angle to S .

In thermal equilibrium S is either negative or zero (Antonov’s rule [18]). The case $S < 0$, which implies $0^\circ < \theta_\infty \leq 180^\circ$, is referred to as partial wetting. It corresponds to drops, surrounded by a microscopically thin film adsorbed at the surface. Classical capillarity predicts the essential features of the shape of such drops. If the drop is

[‡] There is mechanical equilibrium, chemical equilibrium (i.e., the matching of the chemical potential of each species present in the fluid so that the phases are mutually saturated) and thermal equilibrium (i.e., temperature matching) between liquid and gas, so that the gas is the saturated vapour of the liquid. The simultaneous occurrence of mechanical, chemical and thermal equilibrium is referred to as thermodynamic equilibrium.

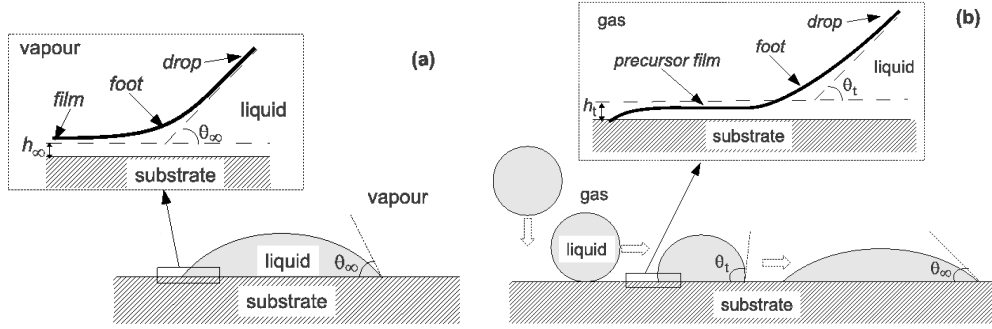


Figure 1. (a) Schematic drawing of a liquid droplet in thermal equilibrium with its saturated vapour and in contact with an inert, flat substrate covered by a thin film of thickness h_∞ at a temperature T below the wetting transition T_W in a bounded system. The inset zooms into the zone near the three-phase contact line and emphasizes that the macroscopic spherical cap is connected with a film covering the substrate via a “foot” region of mesoscopic size (with a height less than 100 nm) where the shape of the liquid-vapour interface is determined by the effective interface potential. (b) Schematic drawing of a spherically shaped droplet of a non-volatile liquid spreading on an inert, flat and unbounded substrate. The inset shows the precursor film emerging during the spreading.

small enough so that gravity can be neglected (i.e., the characteristic length scale of the drop is much smaller than the capillary length χ), the hydrostatic pressure rapidly equilibrates inside the drop; the drop then adopts the shape of a spherical cap in order to obey Laplace’s law (i.e., the pressure difference between the liquid drop and the surrounding vapour is balanced by the surface tension σ_{lv} multiplied by the mean curvature of the drop shape) and the in-plane isotropy. §

Statistical mechanics studies of wetting phenomena in the grand canonical ensemble reveal that in the case of partial wetting (i.e., at bulk liquid-vapour coexistence on the vapour side and at a temperature T below the wetting transition temperature T_w) the substrate is covered by a microscopically thin liquid-like film the thickness h_∞ of which [see the inset in Fig. 1(a)] is temperature dependent and exhibits wetting transitions [18, 32]. In the case of a first-order wetting transition, for $T \rightarrow T_w$ h_∞ jumps to a macroscopic value, whereas h_∞ diverges continuously for a second-order wetting transition (also known as critical wetting [18]). For bounded systems these singularities are smeared out. The spherical cap-like shape of the liquid-vapour interface, which for a suitably large drop is indeed valid far away from the substrate, is distorted in the vicinity of the substrate due to the effective interaction between the liquid-vapour interface and the substrate and smoothly connects to the uniform equilibrium film thickness far away from the drop [18, 33]. The deviations of this actual shape from that of a spherical cap cut by the substrate contribute to the line tension [33–41], i.e., the excess free energy, associated with a line-like inhomogeneity, within the decomposition of the excess free energy into bulk, surface and line contributions [9]. ||

§ Note, however, that the contact angles of partially wetting droplets are very sensitive to various surface defects, surface roughness, contaminants or chemically active sites present on the substrate [16, 26, 31].

|| Instabilities of droplets caused by line tension have been critically discussed in Ref. [42].

2.1.2. Non-equilibrium behaviour. If a droplet is deposited on an initially dry substrate, it is typically not in equilibrium and the equilibrium can be reached only via certain dynamical processes. The way the relaxation towards equilibrium takes place depends significantly on the volatility of the liquid under ambient conditions. If the liquid is volatile, the equilibrium with the ambient gas can be established relatively fast via condensation of vapour onto the substrate. On the contrary, if the liquid is non-volatile under ambient conditions (i.e., if it has a very low vapour pressure), the evolution of the drop shape towards equilibrium will proceed via two-dimensional evaporation and motion of liquid molecules on the substrate surface. Usually, these are much slower processes and in many cases the time required to approach equilibrium after contact with the “dry” substrate can be more than a few hours, or even days.

The pertinent quantity for the dynamics is the initial spreading coefficient

$$S_0 = \sigma_{sg} - \sigma_{lg} - \sigma_{sl}, \quad (4)$$

where σ_{sg} is the surface tension of the dry solid substrate in contact with the gas. The surface tension σ_{sg} is typically larger than σ_{sv} ; assuming that $\sigma_{lg} \simeq \sigma_{lv}$, which is appropriate for an inert gas (i.e., which has a low solubility in the liquid and which does not act as a surfactant) and for temperatures sufficiently far from the critical point, it follows that $S_0 \geq S$. (Note that σ_{sg} is not a measurable quantity; it can be computed assuming the constrained equilibrium that the gas density is constant up to the substrate surface without the formation of a liquid-like wetting film.) The initial S_0 can be positive or negative, but whenever $S_0 < 0$, S is also negative. Hence, for non-volatile liquids and for $S_0 < 0$ the drop will relax toward an equilibrium configuration which displays a non-zero static (equilibrium) contact angle.

2.2. Complete wetting

If the equilibrium spreading coefficient vanishes, i.e., $S = 0$, one has complete wetting. The corresponding equilibrium contact angle of a volatile liquid is zero, i.e., $\theta_\infty = 0$, so that the solid-vapor interface consists of a macroscopically thick wetting layer, which implies that the solid-vapour surface tension equals the sum of the solid-liquid and liquid-vapour surface tension.

For a drop of a non-volatile liquid deposited on a initially dry substrate S_0 is positive (although its equilibrium spreading power $S = 0$), and therefore the drop will spread while preserving its volume. This volume conservation constraint is essential for describing both the spreading dynamics and the final state of non-volatile liquid drops. It explains why in certain situations a non-volatile liquid drop does not spread down to an unbounded film of uniform thickness, but that spreading stops when the drop eventually takes on a “pancake”-like shape of thickness $e(S_0) = a\sqrt{3\sigma_{lg}/(2S_0)}$ (where a is a molecular length [16] specific to nonretarded van der Waals interactions, $a = \sqrt{-A/(6\pi\sigma_{lg})}$, with $A < 0$ being the Hamaker constant). This occurs if short-ranged interactions promote dewetting, even though the overall situation is that of complete wetting. Such structures have been theoretically predicted and analyzed in Refs. [16, 43, 44], and indeed observed later experimentally (see, e.g., Ref. [45]).

3. Spreading of non-volatile droplets

The issue of a non-volatile drop spreading on a substrate from an initial non-equilibrium configuration with $S_0 > 0$ towards its equilibrium shape in situations

in which $S = 0$ has been the subject of extensive experimental and theoretical investigations. The results of this analysis have been reviewed thoroughly in Refs. [16, 26, 31, 46–48]. Here we shall focus only on those main findings which are of interest in the present context. Moreover, we constrain ourselves to the late stages of spreading (and hence, sufficiently small dynamical contact angles) when all transient behaviours and memory-effects of the initial non-equilibrium shape have died out. (Some recent experimental results on the transient inertial regime at very early stages of spreading can be found in Refs. [49, 50].)

In Fig. 1(b) we sketch a typical configuration for a non-volatile liquid droplet spreading on a solid substrate. The drop can be divided into the following two main regions: (i) a macroscopic bulk and (ii) a precursor film, the thickness of which may be on a mesoscopic or a microscopic scale. Note that Fig. 1(b) is schematic and the relative sizes of these regions are not drawn to scale. The *non-equilibrium, time-dependent* parameters θ_t and h_t , which are expected to obey $\theta_t(t \rightarrow \infty) \rightarrow \theta_\infty$ and $h_t(t \rightarrow \infty) \rightarrow h_\infty$, require further discussion. During spreading the shape of the macroscopic part of the drop does not necessarily has to be a spherical cap because spreading is a non-equilibrium process. (Although very often a spherical cap shape is employed in the interpretation of experimental or computer simulations results concerning droplet spreading or dynamic wetting (see, e.g., Ref. [51]) one should keep in mind that it remains an assumption which should be at least checked for validity in each particular instance.) Therefore we shall define the parameters θ_t and h_t without reference to a particular shape. As shown in Fig. 1(b), far away from the substrate the shape of the drop has a negative curvature, while at the precursor film the curvature is approaching zero from above. Therefore there is an inflection point, at a distance from the substrate of the order of the range of the effective interface potential, where the curvature of the shape changes from negative (corresponding to the macroscopic part) to positive (corresponding to the region of the foot and precursor film). Therefore, it is a natural choice to define the macroscopic part of the drop as that part of the shape exhibiting negative curvature up to the inflection point and the “dynamic” contact angle θ_t as the angle formed by the tangent to the drop shape at this inflection point (see also Ref. [52]). The foot of the drop is defined as that part of the drop shape where the curvature is positive and attaining zero from above upon approaching the almost flat precursor film. Accordingly, h_t is defined as the maximum thickness of the film extending ahead of the foot region. Note that for very small or very flat drops (i.e., small equilibrium contact angles) these definitions involving a dynamic macroscopic shape of the drop and a foot region are obviously of limited value because they increasingly depend on the *experimental resolution* and, moreover, the inflection point becomes inadequate as a relevant experimental parameter. In contrast, the definitions of the equilibrium observables θ_∞ and h_∞ remain on solid grounds as long as the amount of liquid is sufficient to limit the fluctuations around a mean shape.

3.1. Non-volatile droplet spreading at macroscopic scales

The key parameter characterizing the spreading of the macroscopic part of the non-volatile drop is the so called capillary number $\text{Ca} = \eta U / \sigma_{lg}$, where U is the velocity of the advancing liquid wedge and η is the viscosity of the liquid. An early experimental analysis of the relation between the dynamical contact angle θ_t and the capillary number has been carried out by Hoffman [53], who studied a forced spreading (with velocities varying over five decades) of a liquid in a capillary, measuring a dynamical

contact angle by a photographic technique. In a series of experiments with silicon oils, he obtained conditions of complete wetting and found a rather universal relation between Ca and θ_t ; in particular, in the limit of low Ca and θ_t he found that his data can be represented as a power law

$$\text{Ca} = \text{constant } \theta_t^\alpha, \quad (5)$$

where $\alpha = 3 \pm 0.5$. Cox [54] treated analytically the rather general problem of one fluid displacing another one on a solid surface for any viscosity ratio and contact angle. He solved the hydrodynamic equations to first order in Ca assuming that the macroscopic wedge with angle θ ends in a zone of molecular extension where slip is allowed. In the complete wetting case and for small contact values his analysis confirmed the result in Eq. (5) with $\alpha = 3$. We note that a relation of this type was first derived theoretically by Fritz [55], but for the slightly different problem of a liquid spreading on a wet surface. In comparison with Cox's analysis, in this case the viscosity of the displaced phase (i.e., vapour) is negligible and the conceptual difficulties arising due to the movement of the contact line on a solid substrate are bypassed by considering a surface covered by a liquid film. A detailed analysis of the relation in Eq.(5) has been carried-out also by Teletzke *et al* [56].

Voinov [57] and Tanner [58] derived analytically the relation in Eq. (5) with $\alpha = 3$ solving the hydrodynamic equations in the lubrication approximation. They have also used the result in Eq. (5) in order to obtain the time evolution of the base radius R_t and the dynamical contact angle θ_t of a spreading droplet of a non-volatile liquid under the assumption that the droplet shape is that of a spherical cap at all times during spreading. In this case R_t and θ_t are coupled due to the constraint of fixed volume V . This leads to the so-called Tanner's laws [57, 58] according to which for sufficiently large R_t and small θ_t these quantities are given by

$$R_t \sim V^{3/10} \left(\frac{\sigma_{lg}}{\eta} t \right)^{1/10} \quad (6)$$

and

$$\theta_t \sim V^{1/10} \left(\frac{\sigma_{lg}}{\eta} t \right)^{-3/10}. \quad (7)$$

Thus the spreading of the macroscopic part of the droplet is rather slow; it would take a very long time to completely spread a macroscopic drop. Note that Eqs. (6) and (7), together with the fixed volume constraint, predict that the final state (i.e., at $t \rightarrow \infty$) of the spreading drop is a two-dimensional gas. However, this is not necessarily so. The validity of the relations (6) and (7), which are based on classical continuum hydrodynamics, breaks down at a crossover time T_0 at which the height of the spreading drop reaches the range of the effective interface potential (which describes the effective interaction between the substrate and the liquid-gas interface).

The behaviours given in Eqs. (6) and (7) have been observed in a number of thorough experimental studies (see, e.g., the detailed analysis of the full shape of a spreading drop by using laser light interferometry reported by Chen and Wada [59] and the review by Marmur [60]). On the other hand, some significant deviations have been observed for spreading liquids with very low viscosity (see, e.g., Ref. [61]). However, such deviations have been explained in Ref. [62] by the influence, at intermediate times, of the dissipation at the macroscopic contact line [63] which is unaccounted for in the hydrodynamic description of spreading.

We finally point out the remarkable feature in Eqs. (6) and (7) that neither the radius nor the dynamic contact angle of the macroscopic part of the droplet depend on the initial spreading power S_0 . This tells that in conditions in which the liquid completely wets the solid the macroscopic spreading turns out to be independent of the wettability (i.e., the value of S_0) of the solid surface. A consistent explanation for this feature is due to Hervet and de Gennes [16,64] who have shown that (i) the macroscopic behaviour described by Eqs. (5), (6) and (7) stems from the interplay of the hydrodynamic dissipation in the wedge of the macroscopic part of the droplet and the “driving force” for spreading provided by the free energy of the drop due to its shape not being the equilibrium one, i.e., a two-dimensional gas or a flat “pancake” (see, c.f., Sec. 3.2.2) and that (ii) S_0 is entirely dissipated in the mesoscopic part of the drop. These arguments have been used further in Refs. [52,65] in order to account for the effects of the line tension on the late-stage (i.e., post-Tanner) spreading of a macroscopic droplet. For simple liquids, the conclusion reached in these references was that in the late stages of spreading a positive line tension is responsible for the formation of pancake-like structures, whereas a negative line tension tends to lengthen the contact line and to induce an accelerated spreading (i.e., there is a crossover to a faster algebraic increase of R_t than in the Tanner stage) [52].

3.2. Non-volatile droplet spreading at mesoscopic scales: mesoscopic films

3.2.1. Experimental evidence. The first reported observation of an “invisible” film spreading ahead of the edge of a macroscopic drop stems from the pioneering work by Hardy [66,67], who studied the behaviour of drops of water, acetic acid, and various other polar organic liquids on clean surfaces of glass and steel. Hardy realized that a film of liquid about one micron thick is pushed out and spreads from a drop, and that, importantly, this process may or may not be followed by spreading of the drop itself. ¶

With the experimental techniques available at that time, a direct observation of such a film – called by Hardy the “primary” film – was not possible. He was able to detect its presence only indirectly, via its lubricating effects, by observing a significant drop of the static friction of the surface both far away and close to the three-phase contact line. Hardy stated that he is unable to conceive a mechanism by which the film is pushed out of the drop and proposed that spreading of the film occurs via a process involving a steady condensation of vapour. +

Two decades later Bangham and Saweris [70], analysing the spreading behaviour of numerous polar and apolar liquids on freshly cleaved mica, have demonstrated that primary films do also occur even in the absence of any vapour in the gas. This suggests that the evaporation/condensation scheme (proposed by Hardy and clearly confirmed by Ref. [69]) is not the only possible physical mechanism producing the film. The

¶ More than half a century later, the observation that the spreading of a drop of water or ethanol depends on the distance from the edge of the substrate led Marmur to the same reasoning that this can only be caused by a very thin film spreading ahead of the drop and interacting with the edge [68].

+ Almost 70 years later, clear evidence for an evaporation-condensation mechanism was reported in Ref. [69], where a microscopic film was detected on a plate physically separated by a narrow gap from the substrate with the sessile drop in a partial wetting state. The thickness profile of this film as a function of the distance from the edge of the droplet was shown to be identical to that of an uninterrupted film formed from a droplet residing on this separated plate. This shows that in this case two-dimensional evaporation out of the three-phase contact line is negligible compared with three-dimensional evaporation.

conclusion drawn from their experiments is that the primary film can also form by surface diffusion of molecules from the edge of the drop. Recently these findings have been re-examined and confirmed [71]. The experiments in Ref. [71] employed pairs of drops of water/alcohol, water/acetic acid, and PDMS/trans-decaline, the first two involving volatile liquids, placed on glass or mica substrates. The occurrence of drop motion has been explained as the result of a surface tension gradient at the solid-gas interface due to the formation of precursor films [71, 72], which, in case of volatile components, form either via an evaporation-condensation mechanism or by spreading on the surface out of one of the drops (PDMS). It was also noted that the thickness of these films is different (although no precise characterization of the thickness was provided): ultra-thin (invisible) in the first case, and mesoscopically thick (visible) in the latter.

In 1964, Bascom *et al* [73] investigated the spreading of the primary film from a more quantitative point of view using ellipsometry and interferometry techniques. They examined the behaviour of various hydrocarbons on clean, horizontal or vertical metal surfaces in the presence of either vapour saturated and vapour unsaturated air. By monitoring the late stages of spreading via ellipsometry it was concluded that a primary film is present in all the cases studied. Making the air saturated or unsaturated with vapour, roughening the surface, and purifying the liquids did not eliminate the occurrence of the film, but only affected the spreading speed. The thickness of the film was found to depend sensitively on the kind of liquid/solid pair under study but generally it amounted to a few hundred Å.

A decade later Radigan *et al* [74] have shown that the appearance of such films is not specific to the drop being *bona fide* liquid. Scanning electron microscopy studies of an inorganic molten glass spreading on a Fernico metal (i.e., a Fe-Ni-Co alloy with a coefficient of linear expansion close to that of hard glass) at 1000° C revealed a spreading film of an average height of the order of one micron. To our knowledge, this was apparently the first publication in which the notion of a “precursor film” has been used.

Finally, Ghiradella *et al* [75] detected a mesoscopic precursor film for a hydrochloric solution rising in a glass vessel on a vertical wall. The existence of the film was demonstrated by monitoring the changes in electrical resistance across the wall. Ausserré *et al* [76] were the first to directly visualise the precursor film with thicknesses of several hundred Å by using polarised reflection microscopy for the spreading of non-volatile high-molecular-weight polydimethylsiloxane (PDMS) on smooth horizontal silicon wafers. The density profiles of these films have been studied by ellipsometry in Ref. [77] and the final stages of spreading of small PDMS droplets in Ref. [78].

3.2.2. Theoretical concepts. We now turn to the theoretical analysis of the time evolution of the mesoscopic part of the drop (see Fig. 1(b)), focusing on scales from ca. 30 Å to 1 µm. At such scales, a continuum picture is still applicable, but certain long-ranged forces become relevant, mainly van der Waals forces for organic liquids, or double-layer forces for water. Accordingly, interfacial tensions alone become insufficient to describe the free energy of the system. An additional free energy term $\omega(h)$ has to be included, which takes into account the interactions between the two interfaces (solid-liquid and liquid-gas for the liquid-on-solid spreading); h is the local film thickness. This additional free energy contribution, known as the effective interface potential $\omega(h)$ [18] has a pressure counterpart, which is the disjoining pressure

$\Pi(h) = -\partial\omega/\partial h$. This was introduced by Derjaguin [79] in order to describe the dynamics of thin liquid films. *

Within the lubrication approximation [40, 79, 80], the spreading of a thin, non-evaporating liquid film on a solid substrate ahead of the macroscopic edge of the drop, which moves with velocity U along the x -direction, is governed by the conservation law

$$\frac{\partial h}{\partial t} = -\frac{\partial}{\partial x}(hU), \quad (8)$$

and the dynamic equation

$$\eta U = \frac{h^2}{3} \frac{\partial}{\partial x} \left(\sigma_{lg} \frac{\partial^2 h}{\partial x^2} + \Pi(h) \right), \quad (9)$$

which holds for mesoscopically thin films in the absence of gravity and surface tension gradients.

Capitalizing on the ideas of Derjaguin [79], Hervet, de Gennes and Joanny [16, 26, 64, 81, 82] and Teletzke *et al* [56] have provided a description of mesoscopic precursor spreading which includes the contribution of the long-ranged forces. This has stimulated a strong activity in the field, both theoretically and experimentally. Following the analysis in Ref. [82], below we shall briefly outline some basic theoretical concepts and results concerning the spreading of mesoscopic precursor films. According to this analysis, explicit results can be obtained in two limiting cases: first, if the velocity U of the macroscopic edge varies very slowly in time (adiabatic case, in which the drift of the edge contributes to the spreading of the precursor), and second, if $U \rightarrow 0$ (diffusive case, in which the motion of the macroscopic edge has stopped and the expansion of the film is controlled solely by the spreading power S_0 and the disjoining pressure).

(A) Adiabatic films. The theoretical analysis of Eqs. (8) and (9) tells that a so-called adiabatic film emanates from a liquid wedge which is advancing with a constant (or slowly varying) velocity U . Under the additional assumptions that curvature effects are negligible and that this film is stationary, i.e., that its shape reaches a stationary shape very rapidly at time scales which are much shorter than the scales at which the velocity of the macroscopic wedge varies (thus the name “adiabatic”), the spreading equation [Eq. (9)] of the film along the x -coordinate reduces to [79, 82, 83]:

$$\eta U = \frac{h^2}{3} \frac{\partial \Pi}{\partial x} = \text{constant}, \quad (10)$$

which renders the film profile. The latter equation can be solved, e.g., for the common case of a non-retarded van der Waals disjoining pressure $\Pi(h) = -A/(6\pi h^3)$, where $A < 0$ denotes the Hamaker constant. For this case a simple analysis [82] shows that for $S_0 > 0$ the distance l_a from the macroscopic wedge to the point at which the height of the adiabatic film is that of a “pancake”, i.e., $h(l_a) = e(S_0) = \sqrt{-A/(6\pi S_0)}$, equals

$$l_a = \frac{-A}{6\pi\eta U e(S_0)} \sim \sqrt{S_0}. \quad (11)$$

Hence, the lateral size of the adiabatic film is proportional to $\sqrt{S_0}$. This shows that, while the macroscopic properties of a spreading droplet are independent of the spreading coefficient, the mesoscopic properties, e.g., the length of the adiabatic film

* Note that $S_0 = \int_0^\infty dh \Pi(h)$, while $S = \int_{h_\infty}^\infty dh \Pi(h)$, where h_∞ is the equilibrium film thickness.

and the thickness of the pancake, do depend on S_0 . In particular, the adiabatic film is longer and thinner the larger S_0 is.

As we have remarked at the end of Section 3.1, in the macroscopic picture [16] the Young capillary force $f_Y = S_0 + \sigma_{lg}(1 - \cos(\theta_t))$ per unit length of the contact line is compensated by the overall viscous force $f_{visc} = \int (\eta U/h) dx$. This viscous force can be split into two parts: the viscous force in the macroscopic wedge which stems from hydrodynamic dissipation in the bulk of the droplet, and the viscous force in the precursor. By integrating both sides of Eq. (10) along the x -axis from the location $x = 0$ of the macroscopic wedge to the tip $x = l_a$ of the precursor film one finds that for arbitrary expressions of the disjoining pressure the viscous force (per length) in the precursor is exactly equal to S_0 . This tells that the entire spreading power S_0 is dissipated in the film. This remarkable result due to Hervet and de Gennes [16, 64] resolved the long standing paradox that under complete wetting conditions the spreading of the macroscopic part of the drop is independent of the value of the spreading power S_0 . This is so because this way the driving force of spreading equals $\sigma_{lg}(1 - \cos\theta_t)$ and it is exactly balanced by the hydrodynamic dissipation in the bulk so that S_0 drops out of the dynamics.

(B) Diffusive films. In view of Eq. (11), the adiabatic films may have a noticeable spatial extent only for very small velocities of the macroscopic wedge. In practice, as soon as the length of the adiabatic film becomes greater than several micrometers, another process comes into play. Since the thickness of this film is not constant spatially, there is a gradient of the disjoining pressure along the film. This causes a non-stationary film – the so-called “diffusive” film – to develop ahead of the adiabatic film. When the length ℓ_t of such a diffusive film becomes sufficiently large, the film turns nearly flat so that curvature effects are negligible. As a result, from Eqs. (8) and (9) one finds that the profile $h(x, t)$ of the spreading diffusive film solves the differential equation [81, 84]

$$\frac{\partial h}{\partial t} = \frac{\partial}{\partial x} \left[\left(-\frac{h^3}{3\eta} \frac{\partial \Pi}{\partial h} \right) \frac{\partial h}{\partial x} \right]. \quad (12)$$

This is a non-linear diffusion-type equation with an effective “diffusion coefficient”

$$D(h) = -\frac{h^3}{3\eta} \frac{\partial \Pi}{\partial h} \quad (13)$$

which depends on the local height of the mesoscopic film. In the presence of dispersion forces $\Pi(h) \sim h^{-3}$ and thus $D(h)$ increases as the height decreases. A straightforward analysis shows [81, 82, 84] that when the diffusive film becomes much longer than the adiabatic one, the length ℓ_t of such a film increases “diffusively”, i.e., in proportion to the square root of time:

$$\ell_t \sim \sqrt{D(e(S_0))t}, \quad (14)$$

where $e(S_0)$ is the thickness of the equilibrium pancake shape of the whole drop. Hence, $D(h = e(S_0))$ is the largest possible value of the diffusion coefficient. In the case of a van der Waals liquid, $D(e(S_0))$ as given by Eq. (13) is comparable with Stokes diffusion coefficient of a sphere of radius $e(S_0)$, i.e., ca. $10^{-9} \text{ m}^2/\text{s}$.

Thus the phenomena occurring at the macroscopic and mesoscopic scales, where hydrodynamics is applicable, can be summarized as follows. In case of complete wetting a macroscopic non-volatile drop spreads very slowly [Eq. (6)] due to the balance between the hydrodynamic viscous dissipation in the bulk and the “driving” Young force (see end of **(A)** above). It gradually empties into a mesoscopically thin

film, which is formed by the lateral gradient of the disjoining pressure during the spreading process and serves as a lubricant for the macroscopic part of the trailing droplet. (This process also removes a singularity in the hydrodynamic dissipation at the three-phase contact line.) The entire initial spreading power S_0 is dissipated by viscous friction in this film. The mesoscopic film flattens as it spreads. When the entire volume of the droplet leaks into the film the spreading process stops and an equilibrium “pancake” is formed. This description remains valid as long as the thickness $e(S_0)$ of this final pancake shape is significantly larger than the molecular size.

3.3. Non-volatile droplet spreading at microscopic scales: ultrathin molecular films

As noted above, the mesoscopic films cannot provide a complete picture for the spreading of a non-volatile liquid droplet. The continuum hydrodynamic description explicitly presumes that the thickness of the liquid film stays within the mesoscopic range which means that the thickness $e(S_0)$ of the pancake should be much larger than the molecular scale. This imposes constraints on the values of the surface tension σ_{lv} and of the spreading power S_0 . Accordingly, the hydrodynamic description might hold for low energy substrates, but may break down for intermediate or high energy surfaces, for which the pancake thickness drops below the size of the liquid molecules. ‡ In this context, the challenging experimental observation [27, 28] that spreading of non-volatile droplets of squalane or PDMS on silicon wafers is accompanied by the occurrence of a film of a *microscopic*, not mesoscopic, thickness called for new experimental approaches and theoretical concepts. These will be reviewed in Sections 4, 5 and 6 below.

4. Experimental studies of spreading of microscopic precursor films

4.1. Molecularly thin precursor films in liquid-on-solid systems

The experimental analysis of films with thicknesses of the order of only several molecular diameters became possible with the advent of advanced experimental techniques such as spatially resolved ellipsometry. Ellipsometry is an optical method allowing for the measurement of the local thickness of very thin films which are deposited on substrates with an optical index of refraction n different from that of the film. If the contrast between the indices of refraction is large [such as for silica or silicon oil ($n = 1.4$ for red light) on a silicon substrate ($n = 3.8$)], effective film thicknesses as small as 0.1 \AA can be measured [28, 85]; the lateral resolution remains usually in the range of micrometers. Here it is important to emphasize that, in fact, ellipsometric measurements yield “effective” thicknesses, which equal the actual thickness multiplied by the local number density (averaged across the film at a certain lateral position) divided by the bulk number density. In other words, the effective thickness is the actual thickness times the ratio $(n_{loc} - 1)/(n_b - 1)$, where n_b is the bulk index of

‡ According to the classification of Zisman [24] there are two main types of solids: (i) hard solids (covalent, ionic, or metallic), and (ii) weak molecular crystals (bound by van der Waals forces, or in some special cases, by hydrogen bonds). Hard solids have “high energy surfaces” ($\sigma_s \sim 0.5$ to 5 N/m), while molecular solids (and also molecular liquids) have “low energy surfaces” ($\sigma_s \sim 0.05 \text{ N/m}$). Here σ_s denotes surface energies, i.e., half of the work needed to separate an infinite piece of material into two half-spaces and take the two emerging solid-vacuum planar interfaces far from each other.

refraction for the liquid and n_{loc} is the local index of refraction (also averaged across the film at a certain lateral position). This local thickness has the property, that it vanishes, if there is no film, i.e., $n_{loc} = 1$. In consequence, effective thicknesses below the molecular diameter can be observed in ellipsometry which signifies that the film becomes a diluted, two-dimensional surface gas, rather than a dense fluid.

Employing spatially resolved ellipsometry with modulated polarization, as developed by Drévilion *et al* [85] and Beaglehole [28], a systematic analysis of spreading speeds of ultrathin precursor films has been carried out by Heslot *et al* [27]. They focused on the temporal evolution of the shapes of rather small drops (with a volume of about $10^{-4}\mu l$) of non-volatile liquids (squalane and PDMS) spreading (in the complete wetting regime) on silicon wafers. First, the authors did not observe a “pancake” as the final stage of spreading but rather they detected a gradual transition to a surface gas due to molecular diffusion on the substrate surface. Second, their analysis revealed a precursor film of nearly molecular thickness the radial extent of which, ℓ_t , increases in time as

$$\ell_t \approx \sqrt{D_1 t}, \quad (15)$$

where the subscript “1” indicates that, distinct from Eq. (13), D_1 is the “diffusion coefficient” related to a molecularly thin precursor film.

Beaglehole [28] analysed the profiles of the microscopic precursor of a spreading drop of siloxane oil on glass, fused silica, and freshly cleaved mica. He also observed that the mean radial extent ℓ_t of the precursor at late stages follows Eq. (15). (Late times mean that they are much larger than the single molecule diffusion time, i.e., the time it would take an isolated molecule to move by diffusion over a distance equal to its diameter, with the lateral extent of the precursor being orders of magnitude larger than this molecular size, yet small enough so that the drop remains large and can act as a particle reservoir.)

Using ellipsometry and X-ray reflectometry in a controlled atmosphere of dry and filtered N_2 , Heslot *et al* [29] (see also Ref. [47]) studied the spreading speed and the number density profiles normal to the substrate of a molecularly thin precursor film emanating from a macroscopic meniscus in a capillary rise geometry in which a vertical silicon wafer covered by a natural oxide is immersed in a light silicon oil (PDMS). They observed a film climbing up the vertical wall the extent of which – after 56 hours – attained macroscopic values of ca. 10 millimeters (see Fig. 2). The film number density varied steplike in the direction normal to the substrate surface. For the major part of the film in lateral direction the effective film thickness was nearly constant with a value of about 6 Å. Near the tip of the film its effective thickness decreases smoothly. Since PDMS is a worm-like polymer with the size of the monomer of the order of 6 Å, the observations have been interpreted such that the major part of the film is a compact monolayer of disentangled PDMS molecules lying flat on the solid surface. The region near the tip, where the measured effective thickness falls to a value corresponding to a submonolayer regime, can be viewed as one populated by a surface gas of PDMS molecules. (Note that this effective thickness can take values below the size of a PDMS molecule.) The lateral extent ℓ_t of the film (denoted as L in Fig. 2) was measured at various times and it was found to be in agreement with Eq. (15) with $D_1 \approx 3 \times 10^{-11} \text{ m}^2/\text{s}$.

Significant progress has been made in Ref. [30] which reports the striking phenomenon of “terraced wetting” (see Fig. 3). Using spatially resolved and time-resolved ellipsometry, it was shown that liquid drops (PDMS or tetrakis(2-

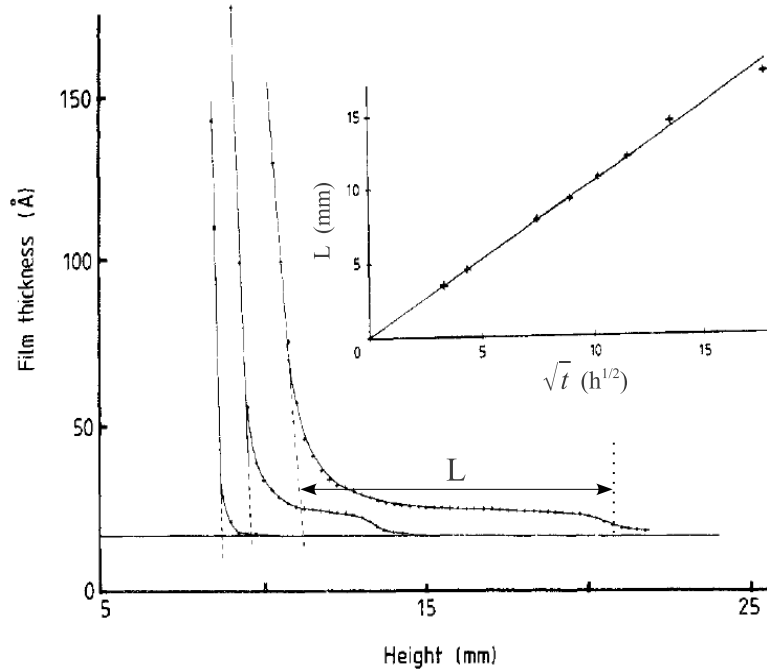


Figure 2. Formation of a low-molecular-mass methyl-terminated polydimethylsiloxane film up a vertical silicon wafer covered with a natural oxide. The curves from left to right correspond to the ellipsometric effective (see the main text) thickness profiles (relative to the surface of the silicon wafer) at 10 min, 10 h, and 56 h, respectively, after the contact of PDMS with the wafer. The x axis is the vertical distance (mm) measured from some fixed point within the bulk liquid; $y = 0$ defines the silicon wafer surface and the base line (i.e., the solid horizontal line at ≈ 18 Å) is the surface of the natural oxide. The reference position, i.e., the end of the macroscopic meniscus from where the extent L of the film is measured, is indicated in each case by a dashed vertical line. Note that the end of the macroscopic meniscus is also moving the vertical plate upwards, but much more slowly than the film; this latter process has not been studied in detail. The vertical dotted line at the right indicates the position of the inflection point in the foot-like region at the advancing edge of the precursor, which is taken to be the point up to where the film extends. Inset: film length L as a function of the square root of time (in units of hours). [Fig. 1 in F. Heslot, A. M. Cazabat, and N. Fraysse, *Diffusion-controlled wetting films*, *J. Phys.: Condens. Matter* **1**, 5793-5798 (1989) (doi:10.1088/0953-8984/1/33/024). Copyright ©1989, reproduced with permission from IOP Publishing Ltd.]

ethylhexoxy)-silane (TK)) spreading on silicon wafers exhibit a strong, dynamical layering in the vicinity of the solid surface so that a spreading droplet advances via a series of distinct molecular layers, such that the k th layer expands proportional to \sqrt{t} with its own “diffusion coefficient” D_k ($\dots > D_{k-1} > D_k > D_{k+1} > \dots$). A similar effect has been observed for spreading of TK in the capillary rise geometry [86]. Since the latter terraced spreading occurred for a system seemingly similar to the one in Ref. [29], for which it was not observed, this behaviour has been further scrutinized in Ref. [87], which focused on the effects of the surface energy on precursor film spreading. It was found that “terraced wetting” occurs on so-called “high-energy” substrates (such as UV-ozone cleaned silicon wafers being used for the experiment immediately

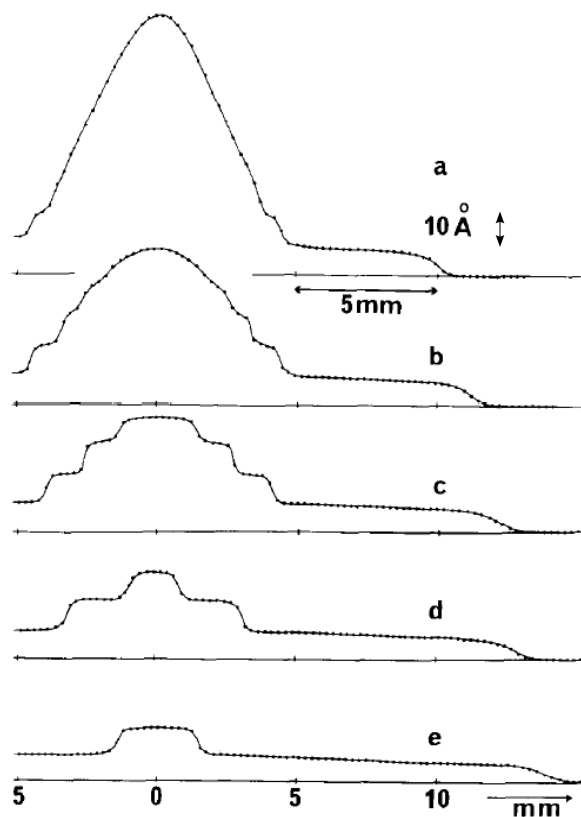


Figure 3. Ellipsometric effective (see the main text) thickness profiles of ultrathin films as function of the radial distance from the center of the drop. The data correspond to a tetrakis(2-ethylhexoxy)-silane (TK) microdroplet with a strongly layered structure (the TK molecule diameter is 10 Å). From top to bottom: 72, 83, 120, 144, and 168 h after deposition. [Fig. 2(b) in F. Heslot, N. Fraysse and A. M. Cazabat, *Molecular layering in the spreading of wetting liquid drops*, *Nature* **338**, 640 - 642 (1989) (doi:10.1038/338640a0). Copyright ©1989, reprinted with permission from Macmillan Publishers Ltd.]

after cleaning). As long as the macroscopic part of the drop acts as a reservoir, up to five such molecular layer were observed, each expanding over macroscopic distances proportional to the square root of time. When the drop starts to run out of material, the top layers were observed to empty themselves into the lower ones, down to the first one. In contrast, for low-energy substrates (such as silicon wafers prepared by monolayer deposition of a fatty acid using the Langmuir-Blodgett technique, see Ref. [87]) typically only a single molecularly thin precursor film has been observed to advance proportional to the square-root of time [87].

The terraced spreading phenomenon has been further studied in Refs. [45, 88, 89] which present a remarkable catalogue of many diverse forms which a spreading "terraced"-shaped droplet can adopt under a variety of conditions for various liquid-on-solid systems. A diversity of profiles of the film thickness has been observed, with either a gradual (if any) variation of the thickness as function of the distance from the macroscopic drop or a rather strong lateral variation. These studies revealed that

the “terraced wetting” phenomenon results from an intricate interplay between the surface energy and friction, and that it occurs for liquids which are non-volatile both in 3D and in 2D. At room temperature this is the case for PDMS oils with a viscosity larger than $0.02 \text{ Pa} \times \text{s}$ and for the silicon derivative TK, and at temperatures below 5°C for squalane.

Perfectly terraced droplets with terraces possessing flat tops and sharp edges have been observed by Daillant *et al* [90,91] for the liquid crystal *8CB* spreading on a (400) silicon wafer and by Betelú *et al* [92] for the liquid crystal *7S5* spreading on an oxide covered (100) Si wafer. Using ellipsometry, for perfluoropolyalkylether (PFPE) films on carbon surfaces Ma *et al* [93] have also observed a complex terraced spreading with an increase of the size of the individual layers proportional to the square root of time, while by using surface plasmon resonance Lucht and Bahr [94] have revealed a terraced structure on gold for the spreading of a liquid-crystalline smectic-A droplet. Similar observations (i.e., terraced spreading or single monolayer spreading of the precursor with an expansion proportional to \sqrt{t}) have been further reported for a variety of complex liquids, such as liquid crystals or alkanes, in contact with bare silicone wafers or ones which are grafted with polymer brushes [91,95–97]. Naturally, in such systems the details of the spreading behavior, such as the prefactor D_1 , differ and the structure of the various spreading monolayers is significantly more complicated.

The influence of the surface energy has been analyzed in detail by Voué *et al* [98] who examined the dependence of D_1 for the precursor monolayer next to the substrate on the surface energy characterized by the so-called critical surface energy γ_c (obtained for alkane series as the abscissa of the point at which the extrapolated linear relation $\cos \theta_\infty$ vs σ_{lv} – the so-called Zisman plot – intercepts the line $\cos \theta_\infty = 1$). By using spatially resolved ellipsometry, these studies showed that D_1 is equal to zero up to a certain threshold value of the surface energy followed by a non-monotonic dependence on the surface energy, exhibiting a pronounced maximum for intermediate surface energies (see Figs. 4 and 5 and Sec. 5).

The effect of the droplet size on the dynamics of such ultrathin films has been studied by Leiderer *et al* [99]. Using the method of optically excited surface plasmon resonance, they determined the density profiles of submonolayer films during spreading of picoliter-volumes of PDMS on a silver substrate. The results showed that the spreading of the film is described by the \sqrt{t} dependence on time which may become significantly slower if the drop is too small to act as a reservoir for the emanating precursor film.

By using scanning micro-ellipsometry and scanning X-ray photoemission spectroscopy, Novotny investigated the spreading behaviour of droplets of perfluoropropylene polymers which are widely used in magnetic recording applications [100]. He observed microscopic precursor films with a sharp edge and spreading in accordance with Eq. (15). He systematically analysed the dependence of D_1 on the molecular weight M and concluded that it can be described effectively by an algebraic law $D_1 \sim M^{-\alpha}$ with $\alpha \approx 1.7$. Fraysse *et al* [101] (see also Ref. [89]) studied the spreading speeds of low molecular weight PDMS precursor films on bare oxidized silicon wafers, used without cleaning, or on wafers bearing loosely grafted trimethyl layers. Their analysis confirmed that the radial extent of the film grows proportionally to the square root of time [Eq. (15)] and it showed that D_1 is inversely proportional to the bulk viscosity $\eta(M)$ of the PDMS liquid. Since for this range of molecular weights the best fit of the PDMS viscosity is given by $\eta(M) \sim M^{1.7}$ [101], the observations made in Ref. [101] appear to agree rather well with the experimental results obtained

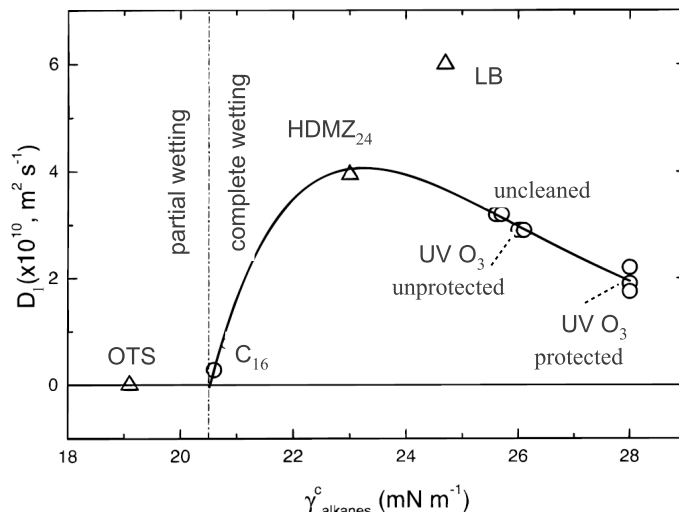


Figure 4. Film diffusion coefficient D_1 for PDMS 20 (molecular mass: 2000; viscosity: 20 cP; surface tension: 20.6 mN m^{-1}) versus critical surface energy ($\gamma_{\text{alkanes}}^c$) of the substrates evaluated for the alkane series. The full line corresponds to the best fit of the data with a theoretical model (Eq. (12) in Ref. [98]). The fit includes only the open circles, see Ref. [98] for details; note that the triangle corresponding to the case labeled by HDMZ₂₄ falls nonetheless on this line. This is, however, not surprising because the surface treatment used to produce this substrate (see below) does not make the HDMZ₂₄ surface too different from those of the original wafers, although it lowers the surface energy due to a trimethyl layer grafted on the native silicon oxide. The data, represented by open circles and triangles, correspond to chemically different and differently treated substrates: “uncleaned” denotes bare wafers used without any cleaning procedure; “UV O₃ unprotected” wafers were UV-ozone cleaned wafers (1 h under a dry O₂ flow plus 20 min under an O₂ flow saturated with H₂O); “UV O₃ protected” wafers were wafers cleaned according to the same procedure but protected after cleaning by aluminum foils and stored under nitrogen in the presence of silica gel to prevent a fast contamination of the reaction sites; “C₁₆” wafers are surfaces obtained by chemical grafting a 3.4 nm thick layer of hexadecyltrichlorosilane; “HDMZ₂₄” surfaces are obtained by exposing an UV-ozone cleaned wafer to hexamethyldisilazane vapour during 24 h at room temperature (this procedure results in grafting a 0.4 nm thick trimethyl layer) and finally, “OTS” wafers are obtained by chemical grafting octadecyltrichlorosilane on a UV-ozone cleaned wafer (this procedure results in a 3.2 nm thick layer). LB denotes a Langmuir-Blodgett wafer which has a behavior completely different from the others showing that the associated ω -tricosenoic acid layers drastically modify the chemistry of the surface. [Fig. 9 in *Dynamics of Spreading of Liquid Microdroplets on Substrates of Increasing Surface Energies*, M. Voué, M. P. Valignat, G. Oshanin, A. M. Cazabat, and J. De Coninck, *Langmuir* **14**, 5951 - 5958 (1998) (doi: 10.1021/la9714115). Copyright ©1998, reprinted with permission from the American Chemical Society.]

by Novotny [100]. Further on, O’Connor *et al* [102,103] and Min *et al* [104] studied the spreading behaviour of PFPE (perfluorinated polyether, terminated with hydroxyl groups), AM2001 (pyperonyl groups), and Ztetraol (propylene glycol ether groups) on silica surfaces as a function of the end group functionality, molecular weight, temperature, and humidity. The square root of time law for the growth of the radial extent of the film has been observed for all liquid-on-solid systems studied

in Refs. [102–104]. But the dependence of D_1 on the molecular weight M turned out to be somewhat weaker, i.e., the observed values of the exponent α seem to be smaller than 1.7. (However, one should keep in mind the merely effective character of this power law.) For example, ellipsometry measurements of ultrathin (i.e., less than 10 Å thick) PFPE precursor film spreading on cleaned silicon wafers with a native oxide layer rendered $\alpha \approx 0.5$ [104], which does not agree with the results of Novotny [100] and Fraysse *et al* [101].

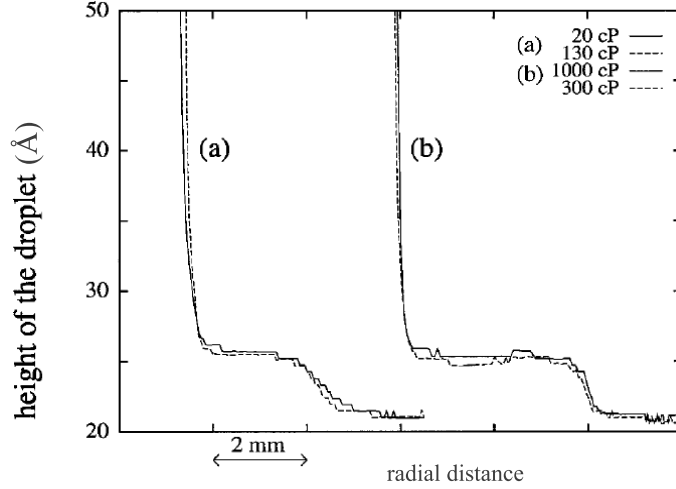


Figure 5. Experimentally determined shapes of several droplets of PDMS of different molecular mass M and polydispersity index I_p (as usual defined as the ratio between the *weight averaged* molecular weight and the *number averaged* molecular weight in a given polymer sample) spreading on one and the same silicon wafer at relative humidity 98%. The profiles are recorded at: (a) 25 min after deposition [solid line: $M = 2000$ g/mol, $I_p = 1.7$; dashed line: $M = 7300$ g/mol, $I_p = 1.10$] and (b) after 40 min [solid line: $M = 28400$ g/mol, $I_p = 1.29$; dashed line: $M = 13000$ g/mol, $I_p = 1.15$]. The legend indicates the corresponding viscosities, in centipoise, of the PDMS oils. Note that the spreading of the macroscopic part of the drop (the macroscopic edge is indicated by the almost vertical lines) is significant, but also seemingly independent of the oil type. The reference plane (silica plus adsorbed water) is at 21 Å. [Fig. 2 in *Molecular Weight Dependence of Spreading Rates of Ultrathin Polymeric Films*, M. P. Valignat, G. Oshanin, S. Villette, A. M. Cazabat, and M. Moreau, *Phys. Rev. Lett.* **80**, 5377 - 5380 (1998) (doi: 10.1103/PhysRevLett.80.5377). Copyright ©1998, reprinted with permission from the American Physical Society.]

This issue has been revisited by Valignat *et al* [105, 106], who studied the molecular-weight dependence of D_1 in Eq. (15) for molecularly thin precursor films of PDMS spreading on hydrophilic oxidized silicon wafers. The wafers were cleaned by oxygen flow under UV illumination and then placed in a measurement chamber for 24 hours. The atmosphere therein contained controlled relative humidity (RH), in order to obtain on the wafer an equilibrated submonolayer of water with controlled coverage, depending on RH. This is motivated by the fact that the substrates used in these experimental studies are chemically heterogeneous and contain different types of surface sites. There are low energy siloxane bridges and high energy, chemically active silanol sites which may form a hydrogen bond with any of the monomers of a PDMS molecule and thus for the latter represent preferred spots of attachment to the surface.

The water molecules have a strong affinity to the silanol sites and effectively screen them, forming molecularly thin islands of water. Hence, exposure to an atmosphere with controlled RH prior to deposition of a PDMS droplet allows one to modify the frictional properties of the substrate by changing the chemical composition of the surface. It was realized that at high substrate friction D_1 is controlled by mesoscopic effects, i.e., by the bulk viscosity $\eta(M)$, and thus as noted above the exponent α can be substantially larger than 1. At moderate RH, i.e., at moderate friction, one observes $D_1 \sim 1/M$ while for very high RH, i.e., low friction, D_1 (and thus the spreading of the precursor) becomes independent of M [105,106] (see Fig. 5, which corresponds to RH = 98 % and shows no significant difference between the full and dashed lines, and Sec. 5).

Furthermore, Villette *et al* [107] focused specifically on the role of water on the spreading of molecular films of PDMS, PDMS with hydroxyl ends (PDMS-OH) and TK on oxidized silicon wafers. Their analysis revealed the dependence of D_1 on RH. In particular, it was realized that for PDMS and PDMS-OH the “diffusion” coefficient D_1 shows a distinctly different linear variation with the relative humidity (and, respectively, with the substrate coverage by water) for RH less than or larger than 70%. For moderate RH, $D_1(RH)$ has a relatively small slope, which at RH $\approx 70\%$ crosses over to a very steep linear dependence on RH. Overall, within the range of 20% to 90% RH, D_1 varies by more than two orders of magnitude, attaining the values observed for mesoscopic precursor films. This agrees well with the observations made by Valignat *et al* [105,106]. Such a remarkable enhancement of D_1 has been explained by the fact that at this value of RH the patches of water on the substrate start to overlap and form a tortuous connected structure on which the spreading of molecules encounters a very low friction. Surprisingly, the dependence of D_1 on RH for TK spreading on hydrophilic substrates appears to be more complicated. Similarly to PDMS and PDMS-OH, D_1 gradually increases up to RH $\approx 70\%$, followed by an abrupt growth. However, at RH $\approx 80\%$ D_1 passes through a maximum and then starts to decrease. At this latter RH one observes signs of a “dewetting transition”, in the sense that the previously distinct first, second and third layers in the terraced shape do no longer occur and only the first layer spreads, while the rest of the drop does not. For RH larger than 85% the behaviour turns into that for partial wetting: while a monolayer precursor film spreads ahead of the drop, the macroscopic part of the drop attains a non-zero equilibrium contact angle.

Within the complete wetting regime, the \sqrt{t} time dependence of a spreading monolayer has also been observed in the case of PDMS on highly polished silicone wafers coated with a self-assembled monolayer of octadecyl-trichlorosilane (OTS) [108]. In this study an interferometric video microscopy technique was employed. See also Ref. [109], in which interferometric microscopy techniques have been employed in order to study the spreading of small drops of very viscous, low-volatile liquids on planar smooth substrates.) The authors have been able to accurately reconstruct the shape of the drop during spreading; from the shape, the volume of liquid in the drop was computed as a function of the time t elapsed since the beginning of spreading. Since under the corresponding experimental conditions the liquid used is practically non-volatile, any change (i.e., decrease) in the volume $V(t)$ enclosed by the drop shape has been attributed to liquid being transferred to a precursor film. Therefore, although such films have not been directly imaged and investigated, their existence and the fact that their linear extent grows in time proportionally to \sqrt{t} could be clearly inferred from the significant changes in $V(t)$ (see Fig. 8 in Ref. [108]).

Finally, we mention several other situations in which spreading ultrathin precursors have been observed for partially wetting liquids. Tiberg and Cazabat [110] have studied the spreading behaviour of non-ionic trisiloxane oligo(ethylene) oxide surfactants on high and low energy surfaces. These surfactant molecules have a peculiar “hammer”-like structure and consist of a compact hydrophobic trisiloxane group sitting as a “hammer head” on an ethylene oxide, which forms a 35 Å long “dangling handle”. It was shown that the spreading of drops of these liquids, if at all, occurs only via an autophobic ultrathin precursor film emanating from the drop (“autophobic” in the sense that the drop “does not wet its own film” but rather remains in a partial wetting state on top of the precursor-covered substrate). On low energy surfaces these surfactants self-assemble over the solid into well defined bilayers the radial extent of which grows proportional to \sqrt{t} , and after a few days in humid atmosphere they cover several square centimeters. The thickness of the precursor is virtually constant (54 ± 2 Å) during the whole spreading process. On high energy surfaces, spreading again occurs via an autophobic precursor, the linear extension of which also grows proportional to \sqrt{t} . But the shape of the vertical cross section of the precursor is now strikingly different having a cone-like shape with a very wide opening angle and a rounded tip rather than a compact organized structure. This aspect has been further studied in Ref. [111], which focused on spreading of various hammer-shaped and linear-shaped surfactants on low, intermediate and high energy surfaces. It was confirmed that spreading of a non-wettable liquid of surfactants proceeds via a ultrathin precursor film with $\ell_t \sim \sqrt{t}$ and only the shape of the vertical cross section of the precursor film depends on the particular choice of the surfactant and of the solid substrate.

4.2. Ultrathin precursor films in metal-on-metal systems

As discussed above, most of the studies of precursor films have been focused on the spreading of liquids on solid substrates. A decade ago, it has been pointed out that microscopically thin films extending over macroscopic distances also occur for wetting in solid-on-solid systems in the so-called Stranski-Krastanov state (crystallites coexisting with a film, see Refs. [112, 113] and references therein). A particular example, which has been the subject of a number of also recent studies [114–119], is that of metal films (Pb, Bi or Pb-Bi alloys) on a metal substrate (mono-crystalline Cu(111), Cu(100) or polycrystalline Cu). As we shall discuss below, these studies have provided evidence for submonolayer precursor films exhibiting the same spreading dynamics (linear extent growing in time as \sqrt{t}) as in the cases of liquid spreading. They allowed a clear identification of surface diffusion through the film as the mechanism of precursor formation and spreading.

At not too elevated temperatures (among these metals, at ca. 544.7 K Bi has the lowest bulk melting point), such systems intrinsically have a very low vapour pressure. The choice of Pb, Bi or Pb-Bi alloys to be deposited on Cu(111) (triangular lattice [114, 116]) or Cu(100) (rectangular lattice [112]) is motivated by the practically negligible bulk solubility of Pb or Bi in Cu. This prevents loss of material via diffusion into the substrate. But there is a good bulk solubility of Bi in Pb, which allows one to prepare alloys over a wide range of concentrations. Moreover, Bi and Pb atoms are very similar in size, which makes the theoretical interpretation of the results easier. In all cases, physical vapour deposition from high-purity metal sources under ultra-high vacuum was used to create thick (i.e., hundreds of nanometers)

overlayers of metal under very well controlled atmospheric conditions. During the preparation of the experiment several cycles of sputtering have been employed to ensure a contaminant-free surface. The investigation of the emerging precursors has also been performed under high-vacuum conditions. The experiment encompassed a combination of scanning Auger electron spectroscopy (SAM) and Scanning Tunneling Microscopy (STM) or Scanning Electron Microscopy (SEM). The former method serves to determine the atomic composition; it has a spatial resolution below one micron and requires ca. 5 min for scanning [114–116]. With the latter methods one can obtain roughly the spatial extent of the film or the shape (i.e., the contact angle) of the Pb or Pb-Bi clusters on the surface.

In the investigations of Pb and of Pb-Bi alloys on Cu(111) [114,116], an initially thick (i.e., hundreds of nanometers) overlayer of metal was gradually heated up to slightly above the melting point of the material (for Pb this is ca. 600 K, and for alloys ca. 538 - 568 K), which led to dewetting and the formation of drops coexisting with a thin film; this configuration was quenched. †† Even in the solid state the droplets are observed to maintain a quasi-spherical shape with just a flattened top; the “dome” rather than “pyramid” shape could be the result of solidification under a rapid temperature quench. This observation allows one to assign an approximate contact angle even for the solidified particles. As reported in Refs. [115,116], for temperatures T in the range $360\text{ K} \lesssim T \lesssim 610\text{ K}$, these contact angles are ca. $40^\circ - 45^\circ$, indicating a partial-wetting situation, with a very weak dependence on temperature and composition. Upon annealing at a desired temperature (note that by varying the temperature one can also control the timescale of the dynamics), by waiting for thermal equilibration and by sputtering off the film (which also ensures a final decontamination), the authors were able to investigate the formation and the spreading of precursor films in contact with liquid drops or solid particles [114–116]. For Bi, a different setup was used, in that the film deposition has been performed on a partially masked substrate, while the remaining steps of the procedure, i.e., annealing and sputtering, were the same. This allowed the study of a precursor formation from a straight contact line [115,116]. Therefore, both straight and circular configurations of the film have been investigated, in addition to the various possible combinations of liquid or solid drops or films.

The results of these experiments revealed that in all cases a precursor film of submonolayer thickness emanates from the drop, and the linear extent ℓ_t of this film obeys the relation given in Eq. (15) with the prefactor D_1 depending on geometry, the metal, the composition of alloys, and temperature. This is very similar to the features observed in the experiments dealing with the spreading of liquids. Somewhat controversially, changes in the temperature dependence of D_1 have been interpreted as to indicate a change in the state of the film between a disordered (fluid) and a partially ordered (solid) structure [115]. Similar changes would occur due to, e.g., a change in the dynamics induced by a partial surface alloying. However, in the case of pure Pb or Bi, the coverage c (i.e., an analogue of the effective film thickness h discussed in Subsec. 4.1), where c is defined such that it takes the value of one (corresponding to a compactly filled monolayer) at the edge of the drop or at the straight contact line, depends strongly on the radial distance x from the edge of the drop or from the straight contact line [see Fig. 6(a)]. In all these cases, dividing the spatial coordinate by $\sqrt{D_0 t}$

†† The authors interpreted these observations as “pseudo-partial” wetting. This confusing nomenclature was clarified later [120].

(D_0 is the corresponding diffusion coefficient of Pb or Bi atoms on the Cu surface) leads to a collapse of the profiles taken at different times t onto a single master curve $\Theta(\lambda = x/\sqrt{D_0 t}; T, \text{metal})$ the shape of which depends on the temperature T and on the materials involved. This scaling is compatible with a surface diffusion mechanism. † The master curve $\Theta(\lambda; \dots)$ does not necessarily have the shape of an error-function, as it would be the case for a simple one-dimensional diffusion process with a fixed concentration source at the origin, but in many cases it exhibits steep drops within certain ranges of coverage [115,116]. This indicates a coverage-dependent diffusion coefficient, which might be caused by certain surface alloying processes as discussed in detail in Refs. [112,113,115,116], but also by attractive interactions between the adsorbed atoms (see Sec. 5). Via a Boltzmann-Matano type analysis [121], from such concentration profiles the coverage dependence of an effective diffusion coefficient $D(c)$ has been obtained. For both Pb and Bi, the resulting diffusion coefficients $D(c)$ have a complex structure, with one [114] or even two minima [115] at intermediate coverages and maxima at high coverages [see Fig. 6(b)]. The positions of the minima are compatible with known surface alloying transitions for Pb or Bi on Cu(111). Similar findings have been reported for films of Pb or Bi on Cu(100) [118]. The results for binary alloys are similar, in the sense that a Pb-Bi film spreads on the Cu(111) substrate, but the rate of spreading seems to be dictated by the slower component and the composition of the alloy varies significantly with the distance from the edge of the drop.

Finally, we note that an interesting extension of this system was studied in Ref. [117], involving two macroscopic films of Pb and Bi, respectively, which are deposited such that they are separated by a small area of the substrate and give rise to precursor films that “collide”. By using SAM, the composition profiles of both Pb and Bi along the direction of mutual approach have been determined. This allows a study of two-dimensional surface interdiffusion of Pb and Bi.

We conclude this section by emphasizing several important features extracted from the experimental analyses of spreading of molecularly thin precursor films.

- (1) Precursor films are omnipresent, even if the liquid droplets only partially wet the solid surface or, in the extreme case, if the drops are actually solidified clusters.
- (2) Precursor films spread from the drop as a result of the competition between the gain in entropy and the balance of the attractive interactions between the fluid molecules and the substrate and the attractive interactions among the fluid molecules. Condensation out of the vapour may, in principle, occur in addition but it is not *condicio sine qua non* for the formation of precursor films.
- (3) Precursor films act as a lubricant for the drops in that the macroscopic part of the drops spreads on a “prewetted” substrate.
- (4) At sufficiently large times (but with the drop still being able to act as a reservoir for the precursor film), the radial extent of the film increases proportional to the square root of time. This dependence holds very generally. Only the prefactor D_1 [Eq. (15)] depends on the particular features of the liquid-on-solid system under study.
- (5) One encounters different types of thickness profiles. (For submonolayer films the coverage is translated into an *effective* thickness, see the discussion of Fig. 2).

† Although Refs. [115,116] mention studies of Pb films at temperatures of 600 K and above, for which the film would be in a disordered state and the drop in the liquid state, no coverage profiles at these temperatures are presented.

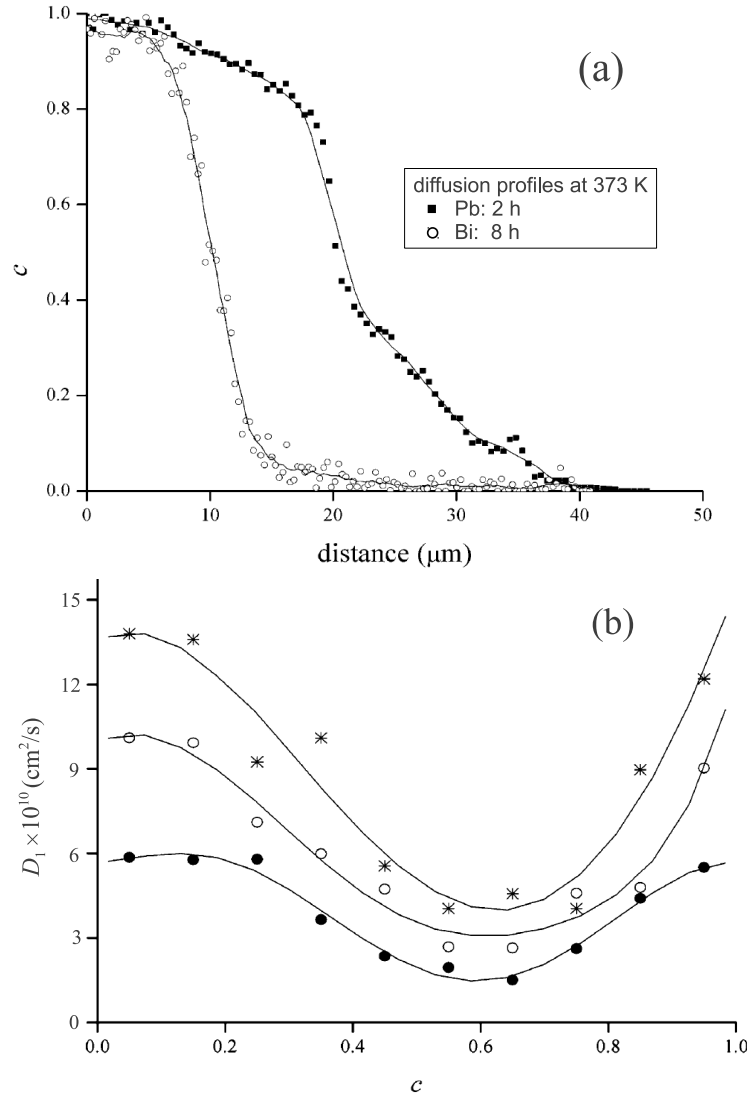


Figure 6. (a) Profiles of the coverage c for Bi (at $t = 8$ h) and for Pb (at $t = 2$ h) on Cu(111) at $T = 373$ K. [Fig. 5 in *Diffusion kinetics of Bi and Pb - Bi monolayer precursing films on Cu(111)*, J. Moon, P. Wynblatt, S. Garoff, and R. Suter, *Surface Science* **559**, 149-157 (2004) (doi:10.1016/j.susc.2004.04.018). Copyright ©2004, reprinted with permission from Elsevier.] (b) Coverage dependence of the diffusion coefficient of Pb on Cu(111) at temperatures 353 K (●), 363 K (○) and 373 K (*). [Fig. 9b in *Pseudopartial Wetting and Precursor Film Growth in Immiscible Metal Systems*, J. Moon, S. Garoff, P. Wynblatt, and R. Suter, *Langmuir* **20**, 402-408 (2004) (doi:10.1021/la030323j). Copyright ©2004, reprinted with permission from the American Chemical Society.] For further details see the main text.

In some instances, molecular-sized precursor films are compact and the thickness profile is laterally constant. In other cases, the thickness along the film varies considerably.

These observations are the basis for formulating a theoretical understanding of the spreading of precursor films.

5. Models for the dynamics of spreading of microscopic precursors

The theoretical analyses of the physical mechanisms underlying the seemingly universal \sqrt{t} -law and the “terraced wetting” phenomenon have followed three different lines of thought.

De Gennes and Cazabat [122] proposed an analytical description of the “terraced wetting” phenomenon, in which the liquid drop on a solid surface was considered as a completely layered structure, the n th layer being a quasi two-dimensional, incompressible fluid of molecular thickness a and with macroscopic radial extent R_n [see Fig. 7(a)]. The interaction energy of a molecule in the n th layer with the solid substrate was taken to be of the general form of a negative, increasing (towards zero) function W_n of the distance $n \times a$ from the substrate.

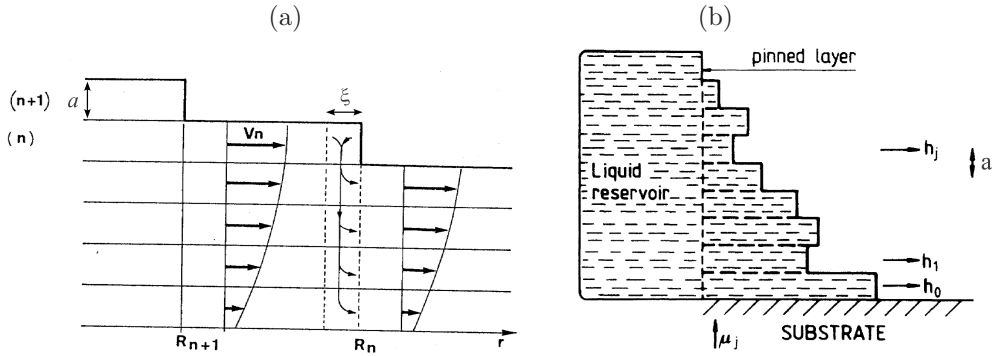


Figure 7. (a) Schematic drawing of the layered structure of a drop as considered in Ref. [122]. In the main text the radial extent R_n of the n th layer is denoted as l_n ; a is the thickness of a layer and ξ denotes the extent of the permeation zone (i.e., where, as indicated, flow occurs along the vertical direction) located at the advancing edge of the topmost layer at a certain R_n and marked by the vertical dashed lines. The velocity field in the n th layer is denoted as V_n . [Fig. 1 in *Spreading of a stratified incompressible droplet*, P.G. de Gennes and A. M. Cazabat, C. R. Acad. Sci. Paris II **310**, 1601-1606 (1990). Copyright ©1990, reprinted with permission from the Académie des Sciences – Institut de France.] (b) Schematic drawing of the horizontal solid-on-solid model considered in Refs. [123–125]. Here the lateral extent of the j th layer is denoted as h_j (as opposed to l_j in the main text) and μ_j (the analogue of W_n as used in Ref. [122]) denotes the interaction with the substrate of the form $\mu_j = \mu_0 f(j)$, where $f(j)$ is a decreasing function of the height j above the substrate and μ_0 is proportional to the Hamaker constant for the system under consideration. At a certain height $j = L$ above the substrate the lateral extent of the corresponding layer is fixed (pinned layer) which mimics the macroscopic wedge which is taken to not evolve with time. Note that for some layers $h_{j+1} > h_j$ as a result of thermal fluctuations. [Fig. 1 in *Dynamics of a microscopic droplet on a solid surface: Theory and simulation*, J. Heiniö, K. Kaski, and D. B. Abraham, Phys. Rev. B **45**, 4409 - 4416 (1992) (doi: 10.1103/PhysRevB.45.4409). Copyright ©1992, reprinted with permission from the American Physical Society.]

Within this model de Gennes and Cazabat [122] considered, similarly to the behaviour observed in smectic systems, two types of flow: a horizontal, outwardly

directed radial particle current and vertical permeation fluxes, one from the neighbouring upper layer and one towards the adjacent layer below. These fluxes are shown to be important only within a thin annulus of small size ξ (comparable to a) near each step, resembling a “permeation ribbon”. Between steps, the viscous effects associated with simple shear dominate. This leads to simple laws for the dilation (or contraction) of the various layers. According to Ref. [122], whenever the distinct layers grow laterally at a comparable rate, they all grow proportional to \sqrt{t} with the proportionality factor $\sqrt{(W_{n+1} - W_n)/\zeta_n}$, where ζ_n is the friction coefficient between the n th and the $(n - 1)$ th layer. This sheds light on the conditions at which “terraced wetting” can occur. Such a phenomenon takes place if in several layers close to the substrate the ratios $(W_{n+1} - W_n)/\zeta_n$ have approximately the same value. If, however, the film closest ($n = 1$) to the solid substrate grows much faster than all the other layers above, i.e., if it decouples from the rest of the drop which then acts as a reservoir for the first layer, this model predicts that the latter one grows proportional to $(t/\ln(t))^{1/2}$ [122]. This is somewhat slower than \sqrt{t} , and terraced wetting does not occur in such a situation.

Within the classical framework of non-equilibrium statistical mechanics an alternative description has been worked out by Abraham *et al* [123, 124] and De Coninck *et al* [125]. Within this approach, an interfacial model for the non-volatile fluid edge has been developed and analysed in terms of Langevin dynamics for the displacements of horizontal solid-on-solid (HSOS) layers $\{l_j\}$ at increasing heights $j = 0, 1, \dots$ from the substrate [see Fig. 7(b), where l_j is denoted as h_j]. These have essentially the same meaning as the layers appearing in the de Gennes-Cazabat model [122], and l_j can be thought of as the radius of the j th layer. The radii and the heights are measured in units of a and thus they are dimensionless.

In the model developed in Refs. [123–125] one has considered the case $f(j) = \delta_{j,0}$ [see Fig. 7(b)], where $\delta_{j,0}$ is the Kronecker-delta, so that the energy $U(\{l_j\})$ of a given configuration $\{l_j\}$ of a one-dimensional interface is described by

$$U(l_0, l_1, \dots, l_L) = \sum_{j=1}^L P(l_j - l_{j-1}) - \mu_0 l_0, \quad (16)$$

where l_0 is the linear extent (in units of a) of the “precursor” film next to the solid substrate, μ_0 is a wall contact potential and the function $P(l_j - l_{j-1})$ describes the free energy contribution due to the non-planar liquid-vapour interface. Explicitly, this latter contribution corresponds to a discretized version of the length of the one-dimensional interface:

$$P(l_j - l_{j-1}) = J \sqrt{1 + (l_j - l_{j-1})^2}, \quad (17)$$

where the parameter J is the surface tension of the one-dimensional interface.

The dynamics of the layers $\{l_j\}$ has been described in Refs. [123–125] by a set of L coupled Langevin equations (recall that l_L is fixed),

$$\zeta \frac{\partial l_k}{\partial t} = - \frac{\partial U(\{l_j\})}{\partial l_k} + f(l_k; t), \quad (18)$$

where ζ is a certain phenomenological “friction” coefficient per unit length of the interface, which is supposed to be the same for all layers, and $f(l_k; t)$ is Gaussian white noise. Note that in this model ζ has a different meaning as compared to the model by de Gennes and Cazabat [122], where ζ is the friction coefficient between adjacent layers and varies with the distance from the substrate; here ζ is associated

with the dynamics of the interface only, it does not depend on the distance from the substrate and it does not account for the dissipation processes occurring in the bulk.

Note as well that the Langevin description of the interface dynamics tacitly presumes that $\{l_j\}$ are continuous variables so that the difference $l_j - l_{j-1}$ is not necessarily constrained to be an integer. This implies that one may encounter two different types of behaviour depending on whether the difference $l_j - l_{j-1}$ is small or large, because the free energy contribution due to the non-planar liquid-vapour interface in Eq. (17) exhibit different asymptotic behaviours. Indeed, in the limit $l_j - l_{j-1} \ll 1$ the function in Eq. (17) is quadratic, i.e., $P(l_j - l_{j-1}) \approx J \{1 + (l_j - l_{j-1})^2/2\}$, while for $|l_j - l_{j-1}| \gg 1$ one has $P(l_j - l_{j-1}) \approx J |l_j - l_{j-1}|$.

This model allows for an analytical analysis, which does yield the extraction of a precursor film as well as “terraced” forms of the dynamical thickness profiles. It predicts that for $\mu_0 > J$ and for sufficiently short precursors (such that the dominant contribution to the surface energy is quadratic), the length of the film increases with time as

$$l_0(t) \sim \sqrt{\frac{(\mu_0 - J) t}{\zeta}}, \quad (19)$$

which resembles the experimentally observed behaviour. For sufficiently long precursors, for which the surface energy increases linearly with the length, the layer next to the substrate grows faster:

$$l_0(t) \sim \frac{(\mu_0 - J) t}{\zeta}. \quad (20)$$

If $\mu_0 = J$, the precursor film advances as

$$l_0(t) \sim \sqrt{t \ln(t)}. \quad (21)$$

Therefore, this model predicts that at very large times the advancing precursor film attains a constant velocity so that the \sqrt{t} -behaviour is only a transient. This inconsistency with the experimental findings can be traced back to the fact that, by focusing on the evolution of the interface and assuming a viscous-type dissipation only at the locus of the interface, the above model neglects the energy dissipation for each molecule within the precursor film as well as dissipation appearing due to viscous flow in the spreading droplet.

To resolve this inconsistency, Burlatsky *et al* [126–128] proposed a microscopic, stochastic model for the spreading of molecularly thin precursors films. Within their approach the film was considered as a two-dimensional hard-sphere fluid with particle-vacancy exchange dynamics [see Fig. 8]. Attractive interactions among the particles in the precursor film were not included into the model explicitly, but introduced in a mean-field-like way. It was assumed that the film is bounded by a HSOS-type interface [123–125], in which the energy parameter J penalizing non-flat interface configurations was considered as a certain (not yet specified in Refs. [126–128]) function of the amplitude of the particle-particle attractions. ‡

The film was taken to be connected to an unlimited reservoir mimicking the bulk liquid (or a macroscopic drop). The rate at which the reservoir releases particles into the film has been related to the local particle density in the film near the nominal contact line and to the strength of the attractive van der Waals interactions between

‡ In Refs. [129,130] an attempt has been made to express the parameter J in terms of the parameters of the interaction between the fluid particles.

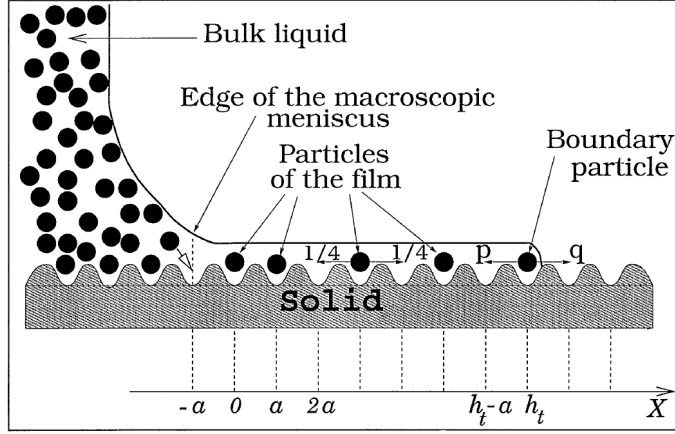


Figure 8. Schematic drawing of a molecularly thin precursor film spreading in capillary rise geometries, i.e., a vertical two-dimensional wall immersed in a liquid bath as considered in Refs. [126–130]. In this effectively one-dimensional geometry the X -coordinate measures the height above the edge of the macroscopic meniscus of the liquid-gas interface and h_t defines the position of the rightmost particle of the film, i.e., of the boundary particle. The latter is subject to a retentive force due to the presence of a HSOS interface bounding the film so that the hopping probabilities p and q of the rightmost particle are asymmetric ($p \leq q$) and are defined by $p/q = \exp(-\beta J)$. Within this model the particles in the film are not subject to any mean force and have equal hopping probabilities for jumping to and away from the meniscus (for a square lattice these probabilities are taken equal to $1/4$). [Fig. 1 in *Microscopic Model of Upward Creep of an Ultrathin Wetting Film*, S. F. Burlatsky, G. Oshanin, A. M. Cazabat, and M. Moreau, *Phys. Rev. Lett.* **76**, 86 - 89 (1996) (doi: 10.1103/PhysRevLett.76.86). Copyright ©1996, reprinted with permission from the American Physical Society.]

the fluid particles and the substrate, in accordance with the standard Langmuir adsorption theory. In contrast to Ref. [122], the model in Refs. [126–128] emphasizes compressibility and molecular diffusion at the expense of hydrodynamic flows. The latter model assumes that the reservoir and the film are in mechanical equilibrium with each other, so that there is no hydrodynamic pressure difference to drive a flow of particles from the reservoir and to push the particles along the substrate and thus away from the droplet. This approach predicted the \sqrt{t} -law [Eq. (15)] for the late time stages of the growth of the molecularly thin film. This law was obtained for the capillary rise geometry and it was found that the density in the film varies strongly with the distance from the reservoir.

Moreover, in Refs. [126–128] the conditions were established under which spreading of the precursor film takes place. It was also suggested that the physical mechanism underlying the \sqrt{t} -law is provided by the diffusive-type transport of vacancies from the edge of the advancing film to the contact line, where they perturb the equilibrium between the macroscopic drop and the film and get filled with fluid particles from the drop.

An extension of the lattice gas model developed in Refs. [126–130] has been proposed and analyzed in Ref. [131] which includes an attractive contribution to the pair interaction between fluid particles, resembling a Lennard-Jones (LJ) potential. The spreading of the monolayer from a reservoir covering a half plane has been studied

as a function of the strength of the attractive pair interaction $U_0 =: W_0 k_B T$ among the particles. The study used both continuous time kinetic Monte Carlo (KMC) simulations as well as a non-linear diffusion equation for the local coverage $c = c(\mathbf{r}, t)$ of the monolayer which is the probability to find at time t a fluid particle in a small area centered at \mathbf{r} :

$$\frac{\partial c}{\partial t} = \nabla[D(c)\nabla c], \quad D(c) = D_0[1 - GW_0c(1 - c)]. \quad (22)$$

This equation has been derived, within a mean-field approximation, from the microscopic dynamics in the corresponding continuum limit. G is a numerical factor which depends on the lattice structure and on the detailed form of the pair interaction, while $D_0 = D(c = 0)$ denotes the one-particle diffusion coefficient on the bare substrate. We note that Eq. (22) has the same mathematical structure as Eq. (12), which describes spreading of mesoscopically thin films so that the former one can be *formally* thought of as being the microscopic analogue of the latter one. However, they differ in their physical origin. In Eq. (22) the coverage dependence of diffusivity arises from the fluid-fluid interactions and the functional form of $D(c)$ encodes the competition between the normal diffusion due to concentration gradients and a local “drift” induced by the mean-field potential due to the particle-particle interactions. In contrast, the diffusivity in Eq. (12) reflects the driving force of the gradients in disjoining pressure, which encodes the effective interaction between the liquid-vapour interface and the substrate.

The model confirms the time dependence $\ell_t = \sqrt{D_1(W_0, c_0)t}$ of the spreading with a prefactor depending on the strength of the interparticle attraction and on the fluid coverage c_0 at the reservoir. The behaviour of $D_1(W_0, c_0)$ agrees with the existence of a covering-noncovering transition separatrix $W_0^{(tr)}(c_0)$ in the (c_0, W_0) plane [129, 130] below which a macroscopic film is extracted from the reservoir and spreads over the substrate, while above it is not extracted. This refers only to the formation of a liquid-like monolayer but does not exclude the formation of a very dilute two-dimensional gas covering the substrate. The coverage of the expanding film as a function of time and distance from the edge of the particle reservoir exhibits a scaling behaviour as function of the scaling variable $\lambda = x/\sqrt{D_0 t}$. These scaled density profiles exhibit qualitatively different structures above and below a threshold value of the interparticle attraction; in particular, above the threshold interaction sharp interfaces form inside the extracted monolayer (see Fig. 9). Such coverage profiles with sharp interfaces are very similar to the experimentally observed ones for the spreading of Bi on Cu(111) [Sec. 4.2], but the cause for their formation is seemingly different. In the former case, they occur because the tendency for clustering becomes dominant for strong inter-particle attraction, which manifests itself as an instability (i.e., a negative diffusion coefficient for a certain range of density values) in the non-linear diffusion equation describing the spreading, while in the latter case a similar instability occurs due to surface alloying of the spreading film.

An interesting lattice gas model for the spreading of ultrathin precursor films, which can be considered as a microscopic version of the continuum model of permeation layers of de Gennes and Cazabat [122], is the one proposed in Refs. [132, 133]. This is an Ising model with nearest neighbour interactions in an external field, provided by the substrate potential, on a cubic lattice of infinite extent along the x and y directions and finite extent along the positive z -direction (in Ref. [133], in units of the lattice spacing $z \in \{1, 2\}$), with local coverage $c(x, y, z) = 0, 1$ if the site is empty (“vacancy”) or occupied by a “particle”, respectively. (The sites

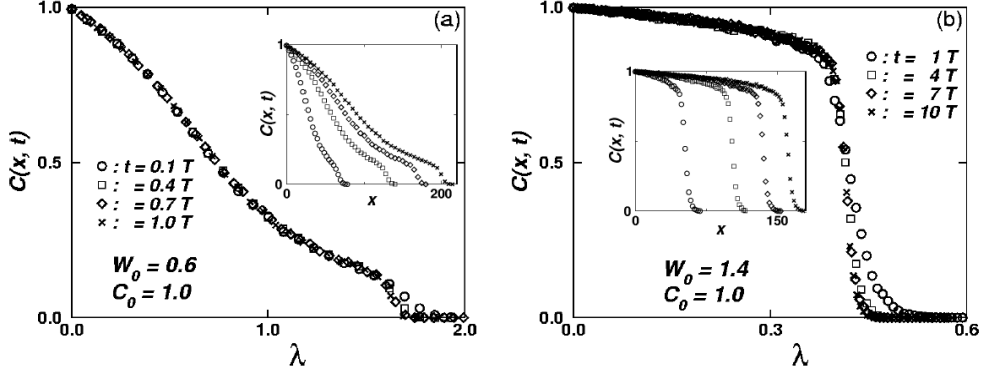


Figure 9. Coverage profiles $c(x, t)$ as functions of the scaling variable $\lambda = x/\sqrt{D_1 t}$ for values of W_0 (a) below and (b) above the threshold value for the emergence of sharp interfaces within the film. The insets show these profiles as functions of the distance x from the edge of the particle reservoir (measured in units of the lattice constant). The time scale $T = 2 \times 10^6$ is measured in units of the average time for a jump attempt of an isolated fluid particle. [Figs. 6(a,b) in *Model for spreading of liquid monolayers*, M.N. Popescu and S. Dietrich, Phys. Rev. E **69**, 061602 (2004) (doi: 10.1103/PhysRevE.69.061602). Copyright ©2004, reprinted with permission from the American Physical Society.]

$z \leq 0$ are attributed to a continuum substrate and cannot be occupied by the fluid.) The model is defined by a configuration-dependent energy at time t given by $\mathcal{H} = -U_0 \sum_{|\mathbf{r}-\mathbf{s}|=1} c(\mathbf{r}, t)c(\mathbf{s}, t) + A \sum_{z=1,2} c(\mathbf{r}, t)/z^3$, $A < 0$. The first term corresponds to a strong nearest-neighbour attraction ($U_0/(k_B T) \gg 1$ in order to ensure low volatility) and the second one corresponds to a van der Waals attraction by the substrate. The dynamics is defined through particle-vacancy exchange rates corresponding to a Kawasaki dynamics augmented by an instantaneous vacancy-particle-exchange process for a particle which would come to be located in the upper layer $z = 2$ exactly above a vacancy in the lower layer $z = 1$. The simulation of the spreading of a precursor, e.g., along the y -direction, employs as initial state a lattice which is half-occupied by fluid, $c(x, y \leq 0, z, t = 0) = 1$, with a fixed coverage $c(x, y = 0, z, t) = 1$ mimicking a fast relaxation of the liquid reservoir at the edge connected to the film. The particles move away from the line $y = 0$ into the initially empty area solely due to the concentration gradients; there is no forcing by the macroscopic film occupying the half space $y < 0$. The advancing edge ℓ_t is defined in the $z = 1$ plane as the largest y position among the rightmost particles in the maximal connected the cluster, i.e., the percolating one in contact with the reservoir. Based on kinetic Monte Carlo simulations it was concluded that the model predicts a compact, first layer precursor spreading which follows $\ell_t \sim \sqrt{t}$ and the emergence of a second layer with a much slower spreading. The mechanism of spreading is the diffusion in the lower layer of a low concentration of vacancies, from the advancing edge towards the “reservoir”. This is coupled to the diffusion in the upper layer of a low concentration of particles in the opposite direction, as well as to the vacancy-particle exchange between the two layers. Therefore, this model points towards a promising direction for studying terraced spreading, which requires simply to relax the constraint $z \leq 2$. However, it is difficult to estimate the ensuing impact on the computational cost (see also Ref. [132]). Moreover, it is unclear whether a non-uniform

structure of the first layer, which would involve particle concentration variations along the spreading direction (see, e.g., Ref. [114]) is compatible with the rules defining the model. This issue arises because the diffusion of vacancies through the high coverage lower layer is much slower than that of particles in the very low coverage upper layer. Thus with increasing extent ℓ_t of the precursor (i.e., the first layer) it is likely that the vacancy-particle exchange mechanism becomes very effective, leading to a vanishing density of vacancies in the first layer.

6. Numerical studies of ultrathin precursors

Computer simulations of various models for liquid droplets spreading on solid substrates have been a very valuable tool in the quest for understanding the mechanisms behind the emergence of terraced spreading and the dynamics of ultrathin precursor films. The methods, which are usually employed, encompass Monte Carlo (MC), kinetic Monte Carlo (KMC), and Molecular Dynamics (MD). They are discussed in detail in many textbooks (see, e.g., Refs. [134,135]). Therefore here we focus strictly on their use for studies of precursor film spreading.

6.1. Monte Carlo simulations

Monte Carlo simulations have been employed to elucidate the emergence of a precursor film (first layer) with a growth behaviour $\ell_t \sim t$ (which disagrees with the experimental observations) within the so-called horizontal solid-on-solid (HSOS) model of non-volatile liquid droplet spreading (see Sec. 5). As discussed above, this model can be solved exactly in certain limiting cases. But although it captures qualitative features of the available experimental results, such as terraced spreading, it predicts a too fast dynamics for the first layer acting as the precursor film. The question arises whether this situation is generic for all the values of the surface tension J and of the parameters characterizing the interaction with the substrate [see Eq. (16)]. If true, this would rule out this model. Otherwise, the too fast dynamics could be a consequence of the approximations made in order to obtain analytic solutions. Monte Carlo simulations of the HSOS model for a liquid wedge have been performed both in two and in three dimensions (i.e., considering a straight edge or allowing for a fluctuating edge for each molecular layer, respectively) for various values of the surface tension and for various cut-off ranges of a van der Waals type substrate potential which decays as $1/z^3$ with the distance z above the planar continuum substrate [136–138]. Except for special values of the parameters (e.g., above, but very near, to the wetting transition line, i.e., close to the temperature at which complete wetting occurs) for which the results are not conclusive due to the very slow dynamics, the simulations provided strong evidence that the first layer indeed spreads with a linear time dependence. This demonstrates that the model is indeed too simplistic. Nonetheless, the time dependence should be interpreted with some caution because these MC simulations have followed the dynamics in “computer time”. This means that each trial move is assumed to take the same average time in order for the time scale of MC steps per lattice site to acquire a physical meaning. This differs from the real time provided by the use of transition rates for various processes, as required by a rigorous KMC method [134]. Later it has been argued that the most likely cause for this discrepancy with the experimental observation is that the model does not account for the energy dissipation associated with the necessary transport of mass from the edge of the drop

to the advancing tip of the precursor [133].

A three-dimensional Ising model for a droplet spreading upon contact with a planar substrate was proposed by Abraham *et al* [139]. In this cubic lattice model, the flat substrate occupies the half space $z \leq 0$, while the sites with $z > 0$ can be either occupied by a fluid particle ($c_i = 1$) or a void ($c_i = 0$), where $c_i \in \{0, 1\}$ denotes the occupation of site i . The model employed a fixed size of the simulation cell (therefore there is a fixed volume available to the fluid) and a fixed number of fluid particles. (These constraints do not play a major role in the case in which three-dimensional evaporation is negligible, as it was the case for the simulations in Ref. [139], see below.) The initial state is that of a lattice approximation of a hemicylindrical drop spanning the whole simulation box along the y -direction, for which periodic boundary conditions have been imposed. The spreading takes place along the x -direction, and the spreading is studied at times for which the advancing edge of the drop or of the precursor (see below) remains far from the boundaries of the simulation box along the x -direction. There is an attractive interaction of strength W_0 between nearest-neighbour fluid particles, and the substrate interacts with the fluid via a van der Waals type potential. Therefore the corresponding Hamiltonian

$$\mathcal{H} = -\frac{U_0}{2} \sum_{\langle i, j \rangle} c_i c_j + A \sum_i \frac{c_i}{z_i^3}, \quad U_0 > 0, A < 0, \quad (23)$$

where $\langle i, j \rangle$ denotes nearest-neighbour sites i and j and $z_i > 0$ is the distance of site i from the substrate at $z = 0$ in units of the lattice spacing. The MC simulations of this model employed a dynamics specified to be a particle-void exchange with Kawasaki rates (see, e.g., Ref. [134]). By varying the ratio U_0/A of the strength of the particle-particle and of the particle-substrate interactions, while keeping the thermal energy sufficiently low in comparison with the particle-particle interactions strength ($k_B T/U_0 = 1/W_0 \leq 2$), such that three-dimensional evaporation was negligible, it was shown that the model exhibits the emergence of terraced spreading. The number of steps and their rate of spreading turned out to be practically independent of the strength of the substrate potential. After a transient time, which can be rather long if the substrate potential is not strong, the spreading of each layer obeyed the \sqrt{t} dependence on the “time” measured in MC steps per lattice site. In this case, the mechanism of mass transport to the film was shown to be a flux of particles along the terraced surface of the drop. This is the microscopic equivalent of the permeation layer in the continuum model proposed in Ref. [122]. However, the maximum lateral extents of the precursor films observed in these simulations are still relatively small (no more than 60 to 80 lattice sites, according to Figs. 1 and 2 in Ref. [139], compared with an initial footprint of the drop of about 30 to 40 sites and a height of about 10 sites). Therefore it is difficult to assess if they can indeed be associated with the *macroscopically* large molecular films observed experimentally. By varying the ratio $k_B T/U_0$ the role of evaporation could be studied. The conclusion was that the qualitative features of the formation and dynamics of the precursor remain the same even if significant evaporation occurs. By varying the number of particles in the drop between 500 and 24000, also the effects of the drop size on the dynamics have been investigated. It was found that there is no significant difference in the behaviour as long as the drop is far from being emptied by the spreading precursors.

A coarse grained description, which emphasizes the mass transfer along the surface of the drop, has been proposed by De Coninck *et al* [140, 141]. This is a restricted solid-on-solid (RSOS) model in which the drop and the film (phase A) in contact with the

flat substrate (W) and a gas phase (B) are described by a set of columns with height values $\{l_0, l_1, \dots\}$ at discrete positions $\{x_i, y_i\}$ on a planar regular lattice, assuming that there are no overhangs. The free energy of a configuration comprises contributions proportional to the areas (or, in a two-dimensional version, the perimeter) of the liquid-vapour, liquid-wall and vapour-wall contact multiplied with the corresponding surface tensions, as well as an additional term $\mu(l)$ modeling a long-ranged effective interaction of the liquid-vapor interface with the substrate; $d\mu/dl$ is the so-called disjoining pressure. The dynamics is introduced as transfers of at most one unit height (thus the name “restricted” SOS model) between neighbouring columns with Kawasaki type rates. Due to the coarse grained nature of the model the MC simulations span much larger time- and length-scales than the ones for the microscopic Ising model discussed above. The results show that the model captures the emergence of terraced spreading [141] as well as spreading of a single layer ahead of the drop [140]. The thickness of these layers depends on the range and the strength of the effective interface potential $\mu(l)$. In all cases, the dependence on time (measured in units of MC steps per site) of the spreading of the precursor is reported to be in agreement with the expected \sqrt{t} -law.

As discussed in Sec. 5, in Refs. [131, 142] a lattice gas model for the spreading of a monolayer precursor in contact with a reservoir of particles mimicking a drop [127, 130, 131] was studied by using continuum time KMC. Due to the focus on the dynamics of the precursor, the computer simulations could explore the dynamics on relatively long time (seconds) and large spatial scales of more than a hundred times the molecular size. They confirmed that the model predicts that the linear extent of the spreading monolayer (provided it does occur) grows in time as \sqrt{t} . These simulations revealed a complex structure of the concentration profiles as a function of the distance from the reservoir, including the emergence of sharp interfaces within the expanding monolayer. A similar model, but one in which the constraint of single-occupancy of a site was relaxed, has been proposed for studying the spreading of a mesoscopically thick precursor films [143]. Numerical simulations of this model in a one-dimensional geometry predict a spreading dynamics of the emerging precursor film which also follows a \sqrt{t} dependence on time.

Finally, we note that in Ref. [144] MC simulations have been reported for the spreading of a polymer droplet of chain-like molecules. They consist of 32 particles with a finitely-extendible, nonlinear and elastic potential between the components of each chain, with a Morse potential as the pair interaction between the components of distinct chains, and with an attractive van der Waals particle-substrate potential. While macroscopic drop spreading (i.e., Tanner’s law) and the early stages of precursor formation have been successfully captured by the simulations, the spreading of the precursor film could not be studied in detail because due to computational limitations the drop size of 128 chains with 32 particles each was too small. Such numerical limitations are expected to become severe if the number of conformational degrees of freedom per molecule is large, in particular as the complexity and the range of the pair potentials are increased.

6.2. Molecular Dynamics simulations for simple or polymeric liquids

A molecular description is provided by MD simulations, in which the particle-particle interactions are specified and the dynamics follows from direct integration of Newton’s equation of motion. In the context of droplet spreading and the formation of precursor

films, MD simulations have been a very useful tool in obtaining direct insight into the molecular details of the physical mechanisms driving the spreading (see Refs. [145–148] and references therein). Before embarking on a summary of the main corresponding developments, a word of caution is yet in order. While the MD method has the advantage of eliminating from the modeling part the numerous assumptions needed as input for the rates which define a MC or KMC dynamics, the method suffers from being computationally extensive and therefore requiring extremely large computer resources (both in terms of memory and CPU time) even for simulating relatively small systems (100 000 particles) over real-time scales of less than one nanosecond. In addition, the actual interaction potentials are rarely well known. The results of MD simulations of droplet spreading should thus be considered as capturing qualitative features, rather than providing a *bona fide* quantitative description. Moreover, they should be carefully scrutinized with respect to finite size effects and time scales which are intrinsically small, in particular if an interpretation for the asymptotic long time behaviour is sought (for an illuminating discussion see, e.g., Refs. [135, 147]).

The first MD studies successfully captured the occurrence of terraced spreading but led to contradictory results for the dynamics of precursors [149–152]. In Refs. [149, 150] fully atomistic MD simulations have been performed, in that both the drop and the substrate were represented as atoms with corresponding inter-particle interactions of a Lennard-Jones form with a cut-off range of the order of the atomic diameter. The various potential parameters characterize the fluid-fluid, fluid-solid, and solid-solid pair interactions, and they are chosen such that at the temperature of the simulations most of the fluid is in the liquid state and that the solid maintains its initial crystalline fcc structure with a (100) plane exposed to the liquid. Due to the aforementioned computational constraints, the size of the system was very small: 4000 particles for the fluid and 9000 particles for the solid, which corresponds to five atomic planes. By varying the strength of the liquid-solid interactions, while keeping the fluid-fluid ones fixed, the simulation explored various wetting regimes. In Ref. [150] an additional strong bonding was introduced between pairs of fluid particles, mimicking diatomic molecules; this sheds light on the influence of the size of the fluid particles on terraced spreading. The results provide clear evidence for the occurrence of terraced spreading as well as for layering inside the core of the drop but still within the liquid state. As intuitively expected, the number of distinct layers increases with increasing strength of the solid-fluid interactions. In these MD simulations the atomic liquid was fairly volatile, whereas the diatomic molecules were practically non-volatile. The simulations revealed that for very strong substrate-fluid interactions the vapor played some role in the formation of the precursor, but by comparing with the case of diatomic molecules it turned out that this evaporation-condensation process is a subdominant effect. However, in all cases studied the precursor film associated with the liquid layer next to the substrate showed a much slower spreading, i.e., $\ell_t \sim \sqrt{\ln(t)}$, than the one observed experimentally and predicted theoretically. This result was puzzling, as it apparently was not a finite-size effect: simulations with twice as many fluid particles reproduced the same behaviour [150].

The MD studies in Refs. [151, 152] considered the case of an atomic fluid as well as that of a binary mixture of single particles, acting as a solvent, and chain molecules. The latter consist of two, four, or eight single particles interconnected by a stiff, isotropic harmonic oscillator potential. All particles are taken to interact via Lennard-Jones potentials and they are in contact with a homogeneous impenetrable substrate which additionally interacts with the particles at a distance z from the substrate via a

van der Waals type potential A/z^3 , $A < 0$. In Ref. [152] the impenetrability condition is implemented by a strongly repulsive term in the substrate-particle interaction $A/z^3 + B/z^9$, $A < 0$, $B > 0$. This substrate potential follows from integrating over a half-space the pair potentials between substrate and fluid particles. Concerning the leading term this is equivalent to carrying out the corresponding discrete sum of pair potentials as used in Refs. [149, 150]. The simulations, performed at temperatures at which evaporation is negligible, have shown that for atomic or diatomic molecules a precursor film occurs in most of the cases, while for longer molecules with orientational degrees of freedom layering and terraced spreading occur only if the strength of the attractive part of the substrate potential is above a threshold value which depends on the chain length. In contrast to the results reported before [149, 150], in all cases in which a precursor film occurred its dynamics did show a \sqrt{t} spreading behaviour after a transient due to the precursor formation. This was followed by a slower expansion once the reservoir drop begins to empty. (In Ref. [151] it is pointed out explicitly that the initial spreading with nearly constant speed later crosses over to diffusive spreading, in turn followed by a slower regime once the macroscopic drop has emptied into the film.) Concerning the studies in Refs. [149, 150], the discrete structure of the substrate consisting of particles of the same size as the one of the fluid particles, the strong substrate-fluid pair interactions, and the moisture of the substrate due to significant evaporation-condensation processes have been surmised [151] to be the most likely sources for the significant difference between the results of Refs. [149, 150] and Refs. [151, 152].

The issue of the dynamics of the precursor spreading has been further investigated with MD simulations in Refs. [153, 154]. These studies employed the same atomistic representation of the substrate as in Refs. [149, 150] with a cut-off for all Lennard-Jones pair potentials at a distance equal to 2.5 times the fluid core size, but with an additional A/z^3 contribution to the resulting substrate potential. However, these studies used chain molecules consisting of 8 or 16 atoms, bound together by a confining pair potential. This led to negligible evaporation and eliminated the similarity in size between the species forming the solid and the fluid, respectively. The simulations revealed the formation of a well-defined first layer precursor film, as well as up to three additional layers spreading much slower than the first one. The dynamics of the first layer shows a clear \sqrt{t} behaviour, which therefore indicates that the behaviour $\ell_t \sim \sqrt{\ln(t)}$ reported previously must be related to the size of the fluid particles used there. It was speculated that due to the compatibility in size the fluid particles in the previous MD simulations are trapped for long times in the local minima of the corrugated substrate potential, which leads to a slow motion along the surface and a correspondingly slow spreading, whereas the chain molecules are incommensurate with the distribution of minima in the corrugated substrate potential and therefore can move easily along the surface [145, 153, 154].

The reason for the slow $\sqrt{\ln(t)}$ spreading behaviour has been finally clearly identified by the MD study in Ref. [155]. It revealed the substrate as being porous, which occurs for specific choices of the lattice constant of the substrate and of the core-size of the fluid particles; they are both implicitly fixed by the choice of the parameters in the Lennard-Jones pair potentials of the substrate and the fluid particles, respectively. The study employed an atomic fluid and a discrete representation of the substrate as atoms forming a lattice. By varying the parameters in the various Lennard-Jones pair potentials, the size of the initial drop, the structure of the substrate lattice [(fcc) or (sc) lattices], and the type of thermostat employed in

the simulations (see Ref. [135]), the authors convincingly showed that in all situations when the precursor film occurs (i.e., for a sufficiently attractive substrate potential and for a sufficiently large drop) its spreading dynamics follows the \sqrt{t} time dependence if the substrate is *impenetrable* [see Fig. 10(a)] and if the drop acts as a reservoir. All the other parameters (including the evaporation-condensation processes) influence only the prefactor in this dependence [see Eq. (15)]. In contrast, for the parameters similar to those used in the studies in Refs. [149, 150], the fluid penetrates into the solid [see Fig. 10(b)] and this indeed gives rise to a much slower spreading which is compatible with a logarithmic time dependence.

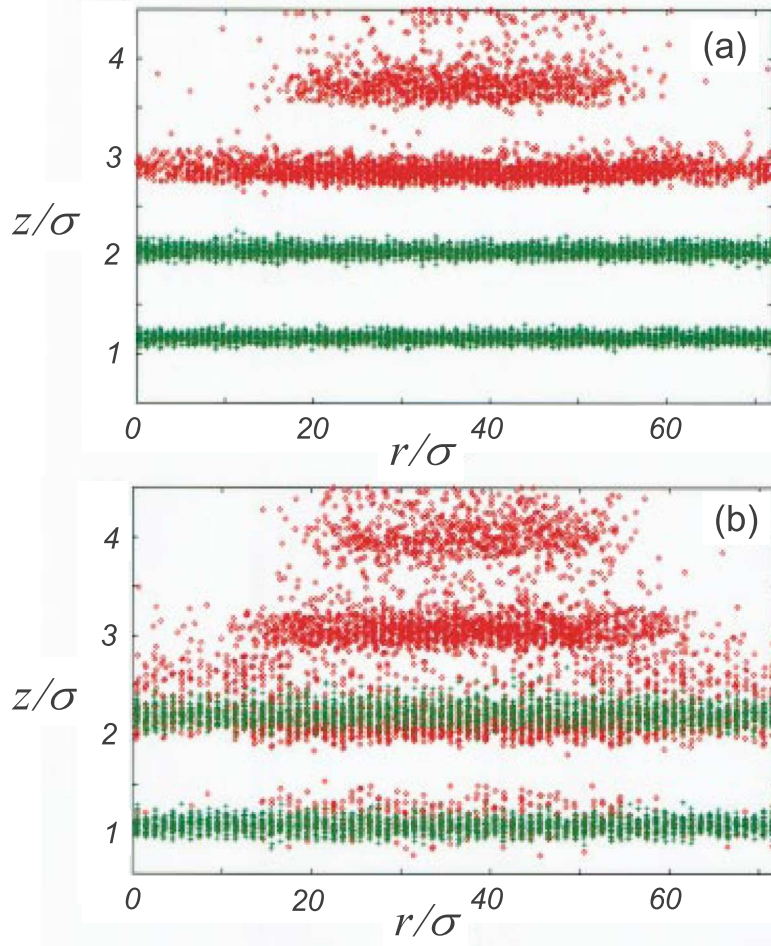


Figure 10. The two uppermost layers of a solid (green) in contact with a fluid drop (red) forming layers, too. In contrast to a solid with nearest-neighbour distance $d_{NN} = 2^{1/6}\sigma$ (a) (where σ is the distance at which the fluid-fluid interaction potential vanishes), the solid with $d_{NN} = 2^{2/3}\sigma$ (b) allows the fluid particles to penetrate the solid which thus acts like a porous material. [Fig. 4(a,b) in *Simulating the spreading of a drop in the terraced wetting regime*, S. Bekink, S. Karaborni, G. Verbist, and K. Esselink, Phys. Rev. Lett. **76**, 3766 - 3769 (1996) (doi: 10.1103/PhysRevLett.76.3766). Copyright ©1996, reprinted with permission from the American Physical Society.]

Further MD studies focused on the case of chain-like molecules, which is closer to experimental situations involving the spreading of polymeric oils. The authors of Ref. [156] employed chain-like molecules, one end of which interacts with the substrate differently than all the other elements of the chain, as it occurs in the case, e.g., of OH terminated PDMS. The MD simulations results revealed that chains which have a preference for being oriented perpendicular to the substrate (this is controlled by adjusting the interaction potential between the modified end element and the substrate in such a way that the minimum of this potential occurs at a distance from the substrate twice as large as that corresponding to the other elements of the chain), lead to a more enhanced lateral structure of the precursor film than chains which prefer to lie flat on the substrate [156]. Although in both cases the dynamics of the emerging monolayer precursor films agrees with the \sqrt{t} behaviour, the prefactor corresponding to the former case is significantly smaller, which is intuitively expected for an enhanced in-plane structuring.

The role of the particle size and of the substrate potential was further explored with MD simulations of binary mixtures with an equal number of chain-like molecules consisting of 8 and 16 atoms, respectively, for which the interactions with the substrate atoms are chosen such that the 16-atom molecules are completely wetting the substrate, while the 8-atom molecules interaction with the substrate is tuned from a partial- to a complete-wetting behaviour [157]. A precursor film with the expected \sqrt{t} dynamics is observed in all cases because one component, i.e., the 16-atom chains, is in the complete wetting regime. The spreading speed lies between the ones of the pure components. As expected, the monolayer precursor is enriched by and the next layer depleted of the 16-atom chains as long as the interaction of the 8-atom chains with the substrate maintains a strength leading to partial wetting. Similar conclusions have been drawn from recent [158] much larger scale MD simulations (300 000 atoms, interacting according to Lennard-Jones potentials) of hemi-cylindrical droplets consisting of either pure 10-, 40-, and 100-atoms chains, respectively, or mixtures of them.

Large scale and long times MD simulations, which allow a simultaneous study of both droplet spreading and precursor film formation and spreading, have been performed in order to investigate the role played by various details, such as the atomic versus a homogeneous structure of the substrate, the type of thermostat algorithm used, the initial shape of the drop, or the size of the substrate [147]. The conclusion is that the computationally most effective method is to use a continuum representation of the substrate, if the porosity of the substrate (see, e.g., Ref. [155]) or substrate alloying (see, e.g., Refs. [159, 160]) are expected to be irrelevant, and to use a thermostat coupling which decays rapidly with the distance from the substrate. The study in Ref. [147] reports the formation of precursor films only for parameters of the LJ pair-potentials which ensure complete wetting of the substrate by the liquid of chain-like molecules. This is in agreement with similar observations made in Refs. [146, 158], but it leaves open the question why such films do not occur in partial wetting situations, which is in contrast to the experimental observations (see Sec. 4.2) and to the MD simulations results for metal on metal systems (see, c.f., Sec. 6.3). Whenever the precursor occurs, its spreading dynamics *at sufficiently long times* is clearly compatible with a \sqrt{t} time dependence for as long as the drop acts as a reservoir and the advancing edge of the film is far from the edges of the substrate. The speed of spreading decreases with the length of the chain-like molecules. Similar conclusions have been reached in MD simulations of a nano-sized droplet with LJ pair potentials spreading on a

substrate in the complete wetting case [161]. Additionally, this latter study emphasizes a comparison with the case of strongly forced wetting occurring when a drop with a non-zero vertical velocity hits a flat impenetrable substrate. In this case inertial terms are actually dominant: the drop spreads and retracts several times before reaching the equilibrium state. Precursor films do not occur because their kinetics is too slow at the time scales imposed by the external driving.

The question of the influence of substrate corrugation, i.e., the periodic lateral variation of the substrate potential due to the crystalline structure of the top layer of the substrate, on the dynamics of the precursor remains basically open. If one would investigate the spreading of a colloidal suspension, corrugation could indeed be completely switched off, because for the big colloids the substrate is *de facto* not corrugated; however, for MD simulations of molecular liquids or metal-on-metal systems, this is not the case. The studies in Refs. [155] and [147] clearly show two limiting cases, one in which the influence of the substrate corrugation is very significant (Ref. [155]), the other in which it plays a minor role (Ref. [147]). We are not aware of any systematic MD studies of the dynamics of the precursor as a function of the lattice structure of the substrate, e.g., concerning the crossover between porous and non-porous substrates. The studies in Ref. [147] indicate that as long as the substrate is not porous the spreading follows the \sqrt{t} . However, for the case of non-porous substrates systematic MD studies of the effects of the lattice geometry and of the lattice spacing on the value of the prefactor are not yet carried out.

An interesting approach for resolving the issue of volatility in MD simulations has been proposed recently in Ref. [162], where the authors use a quarter of a cylindrical liquid drop confined by a rectangular wedge formed by two atomistic semi-infinite fcc walls (minus their overlap). This quarter of a cylindrical liquid drop is covered by an immiscible fluid of equal density and viscosity, and the confinement is completed by two additional homogeneous walls enclosing the covering fluid; periodic boundary conditions apply in the longitudinal direction. By studying the spreading of the first liquid covered by a second, immiscible one, the issue of volatility is bypassed. Both fluids are modeled as atoms interacting with LJ pair potentials. The interaction with the atomistic walls is described by LJ pair-potentials, too, whereas the interaction of any liquid atom with the other two homogeneous walls is described by a van der Waals type substrate potential corresponding to a wedge formed by two semi-infinite walls (minus their overlap). The spreading of the drop away from the corner of the atomistic wedge is initiated by “turning on” an additional attractive van der Waals substrate potential between the droplet atoms and the bottom, horizontal and atomistic wall, along which the spreading takes place. By varying the strength of this latter substrate potential, the liquid-liquid-substrate system is driven from a partial- to a complete-wetting state. In agreement with the previous results of MD simulations for LJ fluids (composed of atoms or chain-like molecules) [146, 147, 157, 158], only for the complete wetting case a thin precursor film extending in front of the “macroscopic” edge of the drop has been observed. The extension of this film was shown to be in agreement with a \sqrt{t} time dependence, with a prefactor depending on the strength of the substrate potential. By fitting *ad hoc* a power law to the extent of this precursor film close to the partial- to complete-wetting transition point – which is *a priori* unjustified, because in that region the linear extent of the film over the time scale of the simulation is microscopic in size, i.e., a few atomic diameters – it has been claimed that the emergence of precursor films is an indication of a transition from partial- to complete-wetting. While this claim seems to hold for LJ fluids and van der Waals substrate

potentials, it cannot be generalized to other fluid-solid models as it obviously is at odds with the experimental evidence (see Sec. 4.2). As we shall discuss below this is also at odds with the results of MD simulations for other pair potentials, such as for metal-on-metal systems. In these systems ultrathin precursor films, expanding proportional to \sqrt{t} , emerge also in partial wetting situations. This is intuitively expected in view of the equilibrium picture of partial wetting corresponding to drops being in spatial contact with microscopically thin films (see Sec. 1).

Maybe the most important recent MD simulation results in this field are those reported in Ref. [160]. The dependence of the precursor spreading on the size of the drop, taken to be a hemi-cylindrical drop in contact with a homogeneous flat substrate, was studied in both *complete and partial* wetting regimes. For the former, a polymer (chain-like molecules with 10 particles) fluid was used, in contact with a substrate acting on the fluid with an integrated LJ potential. For the latter, an atomistic representation of Pb on Cu(111) was used; the equilibrium contact angle was found to be 33° , which is very close to the experimental observations in Ref. [114]. (We re-emphasize, though, that an extrapolation of MD results to macroscopic scales and predictions of material specific properties deserve caveats.) In both cases the temperature and the parameters defining the potentials have been chosen such that the fluid is in the liquid state and practically non-volatile during the time scale of the simulations. The large scale MD simulations involving up to 78 000 polymer chains and up to 220 000 Pb atoms have provided the following results: (i) In both cases a monolayer precursor film emerges out of the drop and spreads ahead of it. The radius of the precursor film, extending to more than 100 times the drop radius, follows a \sqrt{t} time dependence in both cases; for Pb on Cu(111), the total MD simulation time has corresponded to approximately 4 ns, which is a very long time scale by MD standards. (ii) In both cases, the prefactor in the \sqrt{t} dependence is directly proportional to the square root of the initial radius R_0 of the droplet. Extending this finding to the more common case of a spherical drop, this latter result can be interpreted as a dependence of the speed of the spreading precursor film on the volume of the drop. It remains to be seen if such a dependence turns out to be a finite-size effect due to the intrinsically small spatial scales explored by MD simulations. This is a new challenge for theoretical analyses, which so far have been focused on the case of a large *reservoir-like* drop and a spreading speed which is independent of the drop volume. It remains as an open question why in these MD simulations the precursor film occurs even under partial wetting conditions, whereas in other MD simulations it does not.

6.3. Molecular Dynamics simulations for metal-on-metal systems

The experimental results which have provided evidence for precursor films in metal-on-metal systems (see Sec. 4.2) have stimulated the interest in MD simulations for such systems.

Moon *et al* [163] studied the formation and spreading of precursor films of Ag on Ni(100). The choice of Ag and Ni was motivated by the fact that the inter-atomic interactions in metallic systems consisting of different atomic species can be calculated by using the semi-empirical embedded atom method (EAM), and that such EAM potentials are well established for Ni-Ni, Ag-Ag, and Ag-Ni pairs. The MD simulation employed a hemi-cylindrical Ag drop on an atomistic representation (10 atomic planes) of the Ni(100) substrate. The formation and spreading of precursor films from the already equilibrated Ag drop was studied at the temperatures $T = 800$ K, 900 K

and 1000 K. (At these temperatures the simulated Ag drop is actually in a solid state, according to the phase diagrams obtained from numerical simulations [164]). At all temperatures, a film with submonolayer coverage emerged. The coverage c varied as a function of the position x from the edge of the drop and of the time t . The center of the drop maintained a coverage in between 3 and 4 monolayers, fulfilling its role as a reservoir of particles. The dynamics of the film is compatible with the \sqrt{t} time dependence, as shown by the scaling of the coverage profiles when plotted as function of the scaling variable $x/\sqrt{D_1 t}$. No surface alloying or surface ordering in the precursor film were observed. The scaled profiles showed complex shapes, indicating coverage-dependent diffusion coefficients. A Boltzmann-Matano analysis [114,119] was used to extract the diffusion coefficient as a function of coverage. The results exhibit qualitative features of the diffusion coefficient such as a minimum at intermediate coverages and a maximum at large coverages. This behaviour shares a certain similarity with corresponding predictions of lattice-gas models with particles interacting via simple LJ potentials as proposed in Refs. [126,127,131].

The study of Ag spreading on Ni substrates has been extended by Webb *et al* [165] to include the case of cylindrical liquid Ag droplets brought in contact to and spreading on Ni(111) or Ni(100) surfaces. The MD simulations have been performed at 1200 K and 1500 K, i.e., slightly above and well above the melting point, respectively. The experimental bulk melting temperature of Ag is 1235 K, whereas the MD predictions based on the EAM potentials used in Ref. [165] is 1144 K. The numerical results show that spreading on the two surfaces is practically independent of the (111) or (100) surface structure. At 1200 K as a final state incomplete wetting with a contact angle of ca. 10° has been found. At 1500 K a significant dissolution of the Ni substrate occurred and no precursor film has been observed. This is similar to the results of MD simulations for high temperature Ag drops on a Cu surface [164]). In the simulations at 1200 K no surface alloying and very little substrate dissolution were observed, together with evidence for the formation of a submonolayer precursor film. However, even at – by MD simulations standards long – times of approximately 12 ns the extent of the precursor is extremely small. By analyzing the data only up to 4 - 6 ns one could easily be misled to conclude that no precursor is formed. This further emphasizes the need for extreme care in extrapolating the results of MD simulations towards macroscopic, asymptotic behaviours.

A MD simulation study of precursor films of Pb emanating from liquid Pb droplets in contact with Cu(111) and Cu(100) substrates at 700 K has been reported in Refs. [159,160]. The precursors occur in a state of partial wetting (contact angles of 33° and 18° on Cu(111) and Cu(100), respectively). In both cases the precursor films expand by following a \sqrt{t} time dependence, with a significantly larger prefactor for the Cu(111) substrate. On Cu(100) the precursor is a submonolayer thick and, in agreement with theoretical expectations [112], significant surface alloying is observed. In contrast, on Cu(111) no alloying is observed and the precursor consists of two layers. While the lack of surface alloying seems to contradict the theoretical expectations and the experimental observations [113,114], the occurrence of films thicker than a monolayer seems to agree with the experimental observation of a thick film in equilibrium with drops at temperatures above the melting point of Pb [115].

The results and studies discussed in Section 6.2 have significantly contributed towards the understanding of the microscopic mechanisms of ultrathin precursor film formation and of the structure of these films. They have helped to reveal effects particularly significant for small drops, such as the slowing down of a precursor when

the size of the drop becomes too small to act as a reservoir. This also holds for the apparent absence of precursor film formation over time scales which are long by MD standards, yet too short to be asymptotically long. This demonstrates that great care must be exercised concerning the extrapolation of MD data to the large spatial scales and the long time scales typically explored by experimental studies. These observations also tell that, after all, it is only the careful comparison with experimental data which validates a numerical simulation. Moreover, even in the case of favorable agreement this holds usually only at a qualitative level because there is only limited knowledge of the actual form of the force fields governing drop-substrate systems.

Therefore, the recent report in Ref. [166] of a ultrathin precursor film extending in time by following a power law with exponents varying between $\approx 1/7$ and $1/4$ is surprising. This claim is based on MD simulations of a water drop spreading on a (eventually charged) gold substrate. However, direct inspection of the data reveals that they actually correspond to the spreading of the drop, which consists of a quasi-spherical cap *and a foot region* (see Fig. 1), and not that of a film. [For a macroscopic drop it is indeed well documented that the base radius expands slower than the precursor film (see Secs. 2 and 3).] What the authors observe is, at most, the formation of the foot of the drop but not, as claimed, a precursor film. This assessment stems from the following observations: (i) The film in Fig. 2(a) in Ref. [166] has an extent from the edge of the drop of only three molecules, which renders a power law fitting meaningless. (ii) In the case of the reported “complete wetting” a layered film, with no evidence for a precursor, is formed (see Figs. 1(c) and 2(c) in Ref. [166], for electric field $E > E_s$), while nevertheless Fig. 2(c) therein features an exponent $n(E)$ stemming from a power-law fitting of the extent of a non-existent precursor. (iii) The droplet is too small to act as a particle reservoir for the film. The transverse cross section of the initial droplet contains roughly 120 molecules so that a film even with a very small lateral extent (e.g., of 15 molecules measured from the edge of the droplet) would already consume 25 % of the initial droplet mass. A closer look at the data reveals additional issues associated with the simulated system. After what the authors call full spreading, the “water” § droplet shown in Fig. 1(b) in Ref. [166] exhibits a non-zero (and rather large) contact angle, which is confirmed by Fig. 2(c) therein listing a “partial wetting” state for fields $E < E_s$. This is in conflict with the experimental evidence that a smooth and clean gold surface is completely wetted by pure water [167]. Therefore either the interaction potentials used are not appropriate for capturing the behaviour of the system at macroscopic scales, or the potentials are satisfactory but the wetting behaviour of a nanoscale drop of water is different from that of a macroscopic one in a way which is captured, rather than bypassed, by the MD simulations. In either case, extrapolating the results of these MD simulations towards claims of “resolving the Huh-Scriven paradox” (which occurs only within the framework of macroscopic hydrodynamics) || and of understanding actual electro-wetting experiments is unwarranted.

§ The quotation marks serve as a reminder that in the MD simulations assumptions have to be made about the interaction potentials and about the structure of the liquid, e.g., the formation and the strength of hydrogen bonds characteristic for actual water.

|| The Huh-Scriven paradox is that imposing the no-slip boundary condition at the solid-liquid interface in the case of a three-phase contact line moving over a flat and smooth solid leads to a logarithmic divergence of the rate of viscous dissipation in the fluid as function of, e.g., the vanishing slip length (see Ref. [16]).

7. Recent developments

The rapid development of micro- and nano-fluidics devices and the emergence of more accurate and faster methods of surface characterization and analysis has recently led to a renewed interest in the spreading of small droplets and in the formation and structure of precursor films. For example, a new method for studying the precursor dynamics, called epifluorescence, has been proposed. This is a microscopy technique in which the visible light in the microscope eyepieces is the one emitted, through fluorescence, by the specimen itself upon being exposed to light source with a specific wavelength. It has been applied for a silicone oil (PDMS) drop spreading on a glass substrate [168]. The advantages of this method are a lateral resolution of ca. $0.2\ \mu\text{m}$, which is significantly better than that of ellipsometry, and a fast response allowing for a temporal resolution of ca. 200 ms. In principle such a temporal resolution allows one to study the microscopic details of spreading even of low viscosity liquids, which so far has not been possible. A potential drawback of this method is the need of enriching the liquid drop with a fluorescent dye. This may restrict the choice of liquids, and it may even affect the spreading, if for any reason the dye behaves as a surfactant at the liquid-solid or the liquid-gas interfaces of interest. However, these are technical challenges rather than basic drawbacks and it seems reasonable to expect that an adequate choice of dyes can be found for a variety of liquids.

Tapping mode atomic force microscopy (AFM) has also been employed in recent studies of precursor films [169]. This technique, which provides a lateral resolution down to a few nm while preserving a vertical spatial resolution of less than one nm, had been used previously to study the spreading of drops [170, 171]. By employing a well suited setup, with the AFM repeatedly scanning a region at a certain distance from the macroscopic edge of a quasi-stationary drop, Xu *et al* have been able to detect and monitor a precursor film of a complex polymer [poly(tert-butyl acrylate) brush molecules] spreading on a planar highly oriented pyrolytic graphite substrate (which is graphite with an angular spread between the graphite sheets of less than 1°). The observed dynamic behaviour obeys the generic \sqrt{t} dependence [169]. In contrast, the report based on tapping mode AFM of what is called in Ref. [172] a “precursor” film of nanometer extent at the periphery of a small drop consisting of star-shaped polymers, in contact with a silicon oxide substrate has to be treated with caution. The set-up of this experiment is that of a *dewetting* situation and, as the authors acknowledge, the actual film observed was the one remaining on the surface during dewetting, rather than one emerging from the drops. Therefore, it is likely an equilibrium film instead of a precursor.

The ever increasing computing power and storage capabilities of computers combined with the development of new, efficient methods and algorithms for numerical simulations allow one to explore new types of computer experiments as well as to significantly improve the accuracy of previous results. For example, Ref. [173] employed both MD and Lattice-Boltzmann (LB) simulations in order to study the capillary imbibition and precursor film formation in nanotubes. It has been reported that both types of simulations agree in that a molecularly thin precursor film forms ahead of the advancing meniscus, and the lateral extension of this film grows in time as \sqrt{t} , similarly to the observations for other geometries. This is particularly interesting as in this set-up the position of the meniscus moves with a similar time dependence (i.e., following Washburn’s law), but with a smaller prefactor. Therefore this is a more complex situation, in which the dynamics of the precursor film is more

connected to that of the meniscus rather than being independent of it. Moreover, excellent quantitative agreement has been reported between the results of MD and LB simulations. This opens the perspective of using LB simulations, which allow the exploration of time and length scales inaccessible by other numerical methods, for a variety of other systems.

Finally, we note a recently reported [174,175] surprising example of the formation of a “ultrathin” (i.e., monolayer) precursor film, with a spreading dynamics described well by a \sqrt{t} behaviour. The system is a spheroidal aggregate of cells, the surface of each cell containing a certain level of a cell-cell adhesion agent (E-cadherin molecules), in contact with a glass substrate decorated with a mixture of a cell-adhesion agent (fibronectin) and a non-adhesive component (PEG-poly-L-lysine, PEG-PLL). The behaviour of such cellular aggregates bears strong similarities with that of a viscoelastic liquid drop. Accordingly, a spreading coefficient $S_0 = W_{CS} - W_{CC}$, given by the difference between the cell-cell (W_{CC}) and cell-substrate (W_{CS}) adhesion energies per unit area, can be defined analogously to that of a liquid. By varying the amounts of E-cadherin molecules on the cells surface and fibronectin on the glass substrate, it was possible to change S from negative to positive values. This is the equivalent of a transition from incomplete wetting to complete wetting for a liquid-on-solid system. This was confirmed by the corresponding “wetting” behaviour of the cell aggregates. In the complete wetting regime, in which the glass substrate was fully covered by fibronectin, a precursor film, with a thickness equal to one layer of cells, was observed to spread on the substrate ahead of the cell aggregate. The structure of the film is more compact, i.e., liquid-like for stronger cell-cell adhesion; it turns into a sparse, two-dimensional gas-like configuration as the cell-cell adhesion is weakened. The analogy with the liquid-on-solid systems is completed by the observation of an expansion of the liquid-like precursor film showing good agreement with a \sqrt{t} time dependence.

8. Summary and outlook

It can be easily inferred that the combination of experiment, theoretical analysis, and numerical simulations has led to a good understanding of the mechanisms of the formation and the dynamics of precursor films on homogeneous, planar, smooth substrates. However, in our view even for this most basic case several important questions still await answers:

- What are the necessary and sufficient conditions for a precursor film to emerge during the spontaneous spreading of a (quasi)non-volatile drop? Are these the same for a solid-on-solid system such as the metal-on-metal one discussed in Sec. 4.2?
- A good understanding of the dynamics of mesoscopically thick precursor films is available, and theoretical lattice-gas models seem to capture well the dynamics of ultrathin films. A comprehensive theory, which would deal with all length scales and recover the behaviour of thick and ultrathin films as particular limiting cases remains to be developed.
- The early experiments, and so far the only systematic studies of ultrathin precursors, focused on the case of complete wetting. Apart from Refs. [110,111], we are not aware of a similar systematic experimental study of the partial wetting case. Such results are needed to elucidate the importance of the detailed shape of inter-particle pair potentials as revealed by the MD simulations. As we discussed in Secs. 6.2 and 6.3, the choice of the interaction potentials leads to conflicting results on whether or

not a ultrathin precursor film emerges in partial-wetting situations.

By using KMC simulations of lattice gas models few studies have addressed the issue of ultrathin precursor films spreading on chemically inhomogeneous substrates [105, 106, 176] or upon encountering chemical patterns [177]. But questions such as how precursor films form and spread on chemically inhomogeneous or patterned substrate are yet to be explored systematically. Millimeter-sized drops which are set in motion upon contact with a chemically patterned substrate have been recently studied experimentally [178]. However, the question of formation and dynamics of precursor films, as well as that of their influence on the emerging motion of the drop, was not yet addressed. In thermal equilibrium partially wetting nanodrops coexist with a microscopic film. When placed near topographic or chemical heterogeneities on the substrate surface, they interact with them via this film and therefore they are set into motion [179–183]. This naturally leads to the question of how these dynamic phenomena translate to the case in which a ultrathin precursor film, which spreads ahead of a nanodrop, will interact with such geometrical or chemical structures. For example, one can consider the encounter of a precursor with a small chemical patch, which was addressed briefly in Ref. [184], and how in turn this interaction has an influence on the drop. We note here a recently reported elegant example of such precursor-film mediated interactions, applied to achieve thermocapillary actuation even at microscopic scales [25]. By applying a thermal gradient to a parylene-coated silicon substrate, a ultrathin precursor film emerges out of a heptanol drop. This film mediates both the driving of this oil drop towards a water drop sitting nearby, as well as the encapsulation of the water drop by the heptanol. Once the encapsulation is complete, the composite starts moving along the temperature gradient, and thermocapillary actuation is achieved.

The complexity increases by considering whether or not precursor films occur and, if so, how they spread in situations in which the substrate is responsive. Examples are soft substrates such as in the case of a liquid lens at the interface between two immiscible liquids, or at flexible, hairlike substrate structures. Spreading on curved substrates, such as for a sessile drop on a cylindrical or conical rod [185], as well as on substrates with other types of complex geometries, are issues of significant interest which have barely been studied. For example, the very interesting question of spreading of a drop and the formation of precursor films inside a wedge (corner) have been recently approached using MD simulations [186]. These preliminary results (although suffering from a premature interpretation in terms of a heuristic model presumably applicable to the motion of a three-phase contact line but not to the dynamics of ultrathin precursor films [63]) hint at a wealth of qualitatively new phenomena, such as the coexistence of two-dimensional and one-dimensional precursor films spreading ahead of the “macroscopic” contact line. The occurrence and dynamics of precursor films in situations where a volatile or non-volatile colloidal suspension spreads on a substrate [187] provide further important challenges for theory and for applications of wetting.

Acknowledgements

MNP and SD acknowledge financial support from the Australian Research Council (grant DP1094337). AMC wishes to thank Prof. John Ralston for many helpful discussions.

References

- [1] J. F. Padday, editor. *Wetting, spreading, and adhesion*, New York, 1978. Academic Press.
- [2] P. G. de Gennes, F. Brochard-Wyart, and D. Queré. *Capillarity and Wetting Phenomena: Drops, Bubbles, Pearls, Waves*. Springer, Berlin, 2004.
- [3] V. M. Starov, M. G. Velarde, and C. J. Radke. Wetting and spreading dynamics. In *Surfactant Science*, volume 138. CRC Press, Taylor and Francis Group, 2007.
- [4] M. C. Fuerstenau, G. Jameson, and R.-H. Yoon, editors. *Froth flotation: a century of innovation*, Littleton, Colorado, USA, 2007. Society for Mining, Metallurgy, and Exploration.
- [5] H. von Michaelis, editor. *Innovations in gold and silver recovery: phase IV*, Golden, Colorado, USA, 1989. Randol International.
- [6] T. Young. An essay on the cohesion of fluids. *Philos. Trans. R. Soc. London*, 95:65 – 87, 1805.
- [7] P. S. Laplace. *Mécanique Céleste*. Courcier, Paris, 1805.
- [8] J. Plateau. Experimental and theoretical researches into the figures of equilibrium of a liquid mass without weight. *Phil. Mag. Series 4*, 38:445 – 455, 1869.
- [9] J. W. Gibbs. *The Collected Works of J. Willard Gibbs*. Yale University Press, London, 1957.
- [10] J.S. Rowlinson and B. Widom. *Molecular Theory of Capillarity*. Clarendon, Oxford, 1982.
- [11] J.P. Hansen and I.R. McDonald. *Theory of Simple Liquids*. Academic, London, 1986.
- [12] R. Evans. The nature of the liquid-vapour interface and other topics in the statistical mechanics of non-uniform, classical fluids. *Adv. Phys.*, 28:143 – 200, 1979.
- [13] R. Evans. Microscopic theories of simple fluids and their interfaces. In J. Charvolin, J.F. Joanny, and J. Zinn-Justin, editors, *Liquids at Interfaces*, Proceedings of the Les Houches Summer School Lectures, Session XLVIII, pages 1 – 98. Elsevier, Amsterdam, 1990.
- [14] M. Napiórkowski and S. Dietrich. Structure of the effective Hamiltonian for liquid-vapor interfaces. *Phys. Rev. E*, 47:1836 – 1849, 1993.
- [15] K. R. Mecke and S. Dietrich. Effective Hamiltonian for liquid-vapor interfaces. *Phys. Rev. E*, 59:6766 – 6784, 1999.
- [16] P. G. de Gennes. Wetting: statics and dynamics. *Rev. Mod. Phys.*, 57:827 – 863, 1985.
- [17] D. E. Sullivan and M. M. Telo da Gama. Wetting transitions and multilayer adsorption at fluid interfaces. In C. A. Croxton, editor, *Fluid Interfacial Phenomena*, pages 45 – 134. Wiley, New York, 1986.
- [18] S. Dietrich. Wetting phenomena. In C. Domb and J. L. Lebowitz, editors, *Phase Transitions and Critical Phenomena*, volume 12, pages 1 – 218. Academic, London, 1988.
- [19] M. Schick. Microscopic theories of simple fluids and their interfaces. In J. Charvolin, J. F. Joanny, and J. Zinn-Justin, editors, *Liquids at Interfaces*, Proceedings of the Les Houches Summer School Lectures, Session XLVIII, pages 415 – 497. Elsevier, Amsterdam, 1990.
- [20] A. O. Parry and C. Rascon. The self-interaction of a fluid interface, the wavevector dependent surface tension and wedge filling. *J. Phys.: Condens. Matter*, 23:015004, 2011.
- [21] N. R. Bernardino, A. O. Parry, C. Rascon, and J. M. Romero-Enrique. Derivation of a non-local interfacial model for 3d wetting in an external field. *J. Phys.: Condens. Matter*, 21:465105, 2009.
- [22] A. O. Parry, J. M. Romero-Enrique, and A. Lazarides. Nonlocality and short-range wetting phenomena. *Phys. Rev. Lett.*, 93:086104, 2004.
- [23] L. Pang, D. P. Landau, and K. Binder. Simulation evidence for nonlocal interface models: Two correlation lengths describe complete wetting. *Phys. Rev. Lett.*, 106:236102, 2011.
- [24] W. A. Zisman. Contact angle, wettability and adhesion. In F. M. Fowkes, editor, *Advances in Chemistry Series*, volume 43, page 1. American Chemical Society, Washington D. C., 1964.
- [25] Y. Zhao, L. Fangjie, and C.-H. Chen. Thermocapillary actuation of binary drops on solid surfaces. *Appl. Phys. Lett.*, 99:104101, 2011.
- [26] L. Léger and J. F. Joanny. Liquid spreading. *Rep. Prog. Phys.*, 55:431–486, 1992.
- [27] F. Heslot, A. M. Cazabat, and P. Levinson. Dynamics of wetting of tiny drops: Ellipsometric study of the late stages of spreading. *Phys. Rev. Lett.*, 62:1286 – 1290, 1989.
- [28] D. Beaglehole. Profiles of the precursor of spreading drops of siloxane oil on glass, fused silica, and mica. *J. Phys. Chem.*, 93:893 – 899, 1989.
- [29] F. Heslot, A. M. Cazabat, and N. Fraysse. Diffusion-controlled wetting films. *J. Phys.: Condens. Matter*, 1:5793 – 5798, 1989.
- [30] F. Heslot, N. Fraysse, and A. M. Cazabat. Molecular layering in the spreading of wetting liquid drops. *Nature*, 338:640 – 642, 1989.
- [31] D. Bonn, J. Eggers, J. Indekeu, J. Meunier, and E. Rolley. Wetting and spreading. *Rev. Mod. Phys.*, 81:739 – 805, 2009.

- [32] R. Pandit, M. Schick, and M. Wortis. Systematics of multilayer adsorption phenomena on attractive substrates. *Phys. Rev. B*, 26:5112 – 5140, 1983.
- [33] C. Bauer and S. Dietrich. Quantitative study of laterally inhomogeneous wetting films. *Eur. Phys. J. B*, 10:767 – 779, 1999.
- [34] J.O. Indekeu. Line tension at wetting. *Int. J. Mod. Phys. B*, 8:309 – 345, 1994.
- [35] T. Getta and S. Dietrich. Line tension between fluid phases and a substrate. *Phys. Rev. E*, 57:655 – 671, 1998.
- [36] H. Dobbs. The modified Young’s equation for the contact angle of a small sessile drop from an interface displacement model. *Int. J. Mod. Phys. B*, 13:3255 – 3259, 1999.
- [37] T. Pompe. Line tension behavior of a first-order wetting system. *Phys. Rev. Lett.*, 89:076102, 2002.
- [38] T. Pompe and S. Herminghaus. Three-phase contact line energetics from nanoscale liquid surface topographies. *Phys. Rev. Lett.*, 85:1930 – 1933, 2000.
- [39] L. R. White. On deviations from Young’s equation. *J. Chem. Soc., Faraday Trans. 1*, 73:390 – 398, 1977.
- [40] N. V. Churaev, V. M. Starov, and B. V. Derjaguin. The shape of the transition zone between a thin film and bulk liquid and the line tension. *J. Colloid Interface Sci.*, 89:16 – 24, 1982.
- [41] L. Schimmele, M. Napiórkowski, and S. Dietrich. Conceptual aspects of line tensions. *J. Chem. Phys.*, 127:164715, 2007.
- [42] S. Mechkov, G. Oshanin, M. Rauscher, M. Brinkmann, A. M. Cazabat, and S. Dietrich. Contact line stability of ridges and drops. *EPL*, 80:66002, 2007.
- [43] E. Ruckenstein. Conditions for spreading as single molecules or as a thin planar drop. *J. Colloid Interface Sci.*, 86:573 – 574, 1982.
- [44] J. F. Joanny and P. J. de Gennes. Static structure of wetting films and contact lines. *C. R. Acad. Sci. II*, 299:279 – 283, 1984.
- [45] A. M. Cazabat, N. Fraysse, F. Heslot, P. Levinson, J. Marsch, F. Tiberg, and M. P. Valignat. Pancakes. *Adv. Colloid Interface Sci.*, 48:1 – 17, 1994.
- [46] A.-M. Cazabat. How does a droplet spread? *Contemp. Phys.*, 28:347 – 364, 1987.
- [47] A.-M. Cazabat. Wetting films. *Adv. Colloid Interface Sci.*, 34:73 – 88, 1991.
- [48] M. Rauscher and S. Dietrich. Wetting phenomena in nanofluidics. *Annu. Rev. Mater. Res.*, 38:143 – 172, 2008.
- [49] J. C. Bird, S. Mandre, and H. A. Stone. Short-time dynamics of partial wetting. *Phys. Rev. Lett.*, 100:234501, 2008.
- [50] L. Chen, G. K. Auernhammer, and E. Bonaccorso. Short time wetting dynamics on soft surfaces. *Soft Matter*, 7:9084 – 9089, 2011.
- [51] T. D. Blake, A. Clarke, J. De Coninck, and M. J. de Ruijter. Contact angle relaxation during droplet spreading: Comparison between molecular kinetic theory and molecular dynamics. *Langmuir*, 13:2164 – 2166, 1997.
- [52] S. Mechkov, A. M. Cazabat, and G. Oshanin. Post-Tanner stages of droplet spreading: the energy balance approach revisited. *J. Phys.: Condens. Matter*, 21:464131, 2009.
- [53] R. Hoffman. Study of advancing interface. 1. Interface shape in liquid-gas systems. *J. Colloid Interface Sci.*, 50:228 – 241, 1975.
- [54] R. G. Cox. The dynamics of the spreading of liquids on a solid surface. Part 1. Viscous flow. *J. Fluid Mech.*, 168:169 – 194, 1986.
- [55] G. Fritz. Über den dynamischen Randwinkel im Fall der vollständigen Benetzung. *Z. Angew. Phys.*, 19:374 – 378, 1965.
- [56] G. F. Teletzke, H. T. Davis, and L. E. Scriven. Wetting hydrodynamics. *Rev. Phys. Appl.*, 23:989 – 1007, 1988.
- [57] O. V. Voinov. Hydrodynamics of wetting. *Fluid Dynamics*, 11:714 – 721, 1976.
- [58] L. H. Tanner. The spreading of silicone oil drops on horizontal surfaces. *J. Phys. D: Appl. Phys.*, 12:1473 – 1484, 1979.
- [59] J. D. Chen and N. Wada. Wetting dynamics of the edge of a spreading drop. *Phys. Rev. Lett.*, 62:3050 – 3053, 1989.
- [60] A. Marmur. Equilibrium and spreading of liquids on solid surfaces. *Adv. Colloid Interface Sci.*, 19:75 – 102, 1983.
- [61] G. Sawicki. Dynamic surface phenomena associated with the spontaneous spreading of silicone fluids. In J. F. Padday, editor, *Wetting, Spreading and Adhesion*, pages 361 – 375. Academic Press, New York, 1978.
- [62] M. de Ruijter, J. De Coninck, and G. Oshanin. Droplet spreading: partial wetting regime revisited. *Langmuir*, 15:2209 – 2216, 1999.
- [63] T. D. Blake and J. M. Haynes. Kinetics of liquid/liquid displacement. *Journal of Colloid and*

- Interface Science*, 30:421 – 423, 1969.
- [64] H. Hervet and P. G. de Gennes. The dynamics of wetting: precursor films in the wetting of "dry" solids. *C. R. Acad. Sci. II*, 299:499 – 503, 1984.
 - [65] S. Mechkov, A. M. Cazabat, and G. Oshanin. Post-Tanner spreading of nematic droplets. *J. Phys.: Condens. Matter*, 21:464134, 2009.
 - [66] W. B. Hardy. The spreading of fluids on glass. *Phil. Mag.*, 38:49 – 55, 1919.
 - [67] W. B. Hardy. *Collected Works*. University Press, Cambridge, 1936.
 - [68] A. Marmur. The dependence of drop spreading on the size of the solid surface. *J. Colloid Interf. Sci.*, 78:262 – 264, 1980.
 - [69] V. J. Novotny and A. Marmur. Wetting autophobicity. *J. Colloid Interf. Sci.*, 145:355 – 361, 1991.
 - [70] D. H. Bangham and Z. Saweris. The behaviour of liquid drops and adsorbed films at cleavage surfaces of mica. *Trans. Faraday Soc.*, 34:554 – 569, 1938.
 - [71] P. Bahadur, P. S. Yadav, K. Chaurasia, A. Leh, and R. Tadmor. Chasing drops: Following escaper and pursuer drop couple system. *J. Colloid Interf. Sci.*, 332:455 – 460, 2009.
 - [72] R. Tadmor. Marangoni flow revisited. *J. Colloid Interf. Sci.*, 332:451 – 454, 2009.
 - [73] W. D. Bascom, R. L. Cottington, and C. R. Singleterry. Dynamic surface phenomena in the spontaneous spreading of oils on solids. In F. M. Fowkes, editor, *Contact Angle, Wettability, and Adhesion*, chapter 27, pages 355 – 379. American Chemical Society, Washington, D.C., 1964.
 - [74] W. Radigan, H. Ghiradella, H. L. Frisch, H. Schonhorn, and T. K. Kwei. Kinetics of spreading of glass on Fernico metal. *J. Colloid Interface Sci.*, 49(2):241 – 248, 1974.
 - [75] H. Ghiradella, W. Radigan, and H. L. Frisch. Electrical resistivity changes in spreading liquid films. *J. Colloid Interface Sci.*, 51:522 – 526, 1975.
 - [76] D. Ausserré, A. M. Picard, and L. Léger. Existence and role of the precursor film in the spreading of polymer liquids. *Phys. Rev. Lett.*, 57:2671 – 2674, 1986.
 - [77] L. Léger, M. Erman, A. M. Guinet-Picard, D. Ausserré, and C. Strazielle. Precursor film profiles of spreading liquid drops. *Phys. Rev. Lett.*, 60:2390 – 2393, 1988.
 - [78] J. Daillant, J. J. Benattar, L. Bosio, and L. Léger. Final stages of spreading of polymer droplets on smooth solid surfaces. *Europhys. Lett.*, 6:431 – 436, 1988.
 - [79] B. Derjaguin. On the notion and definition of the value of the disjoining pressure and its role in statics and kinetics of thin liquid films. *Kolloidn. Zh.*, 17:207 – 214, 1955.
 - [80] A. Oron, S. H. Davis, and S. E. Bankoff. Long-scale evolution of thin liquid films. *Rev. Mod. Phys.*, 69:931 – 980, 1997.
 - [81] J. F. Joanny. Dynamics of wetting: Interface profile of a spreading liquid. *J. Theor. Appl. Mech.*, 5 (special issue):249 – 271, 1986.
 - [82] J. F. Joanny and P. G. de Gennes. Upward creep of a wetting fluid: a scaling analysis. *J. Phys. France*, 47:121 – 127, 1986.
 - [83] P. G. de Gennes. The dynamics of a spreading droplet. *C. R. Acad. Sci. II*, 298:111 – 115, 1984.
 - [84] P. G. de Gennes. Spreading laws for microscopic droplets. *C. R. Acad. Sci. II*, 298:475 – 478, 1984.
 - [85] B. Drevillon, J. Perrin, R. Marbot, A. Violet, and J. L. Dalby. Fast polarization modulated ellipsometer using a microprocessor system for digital Fourier-analysis. *Rev. Sci. Instr.*, 53:969 – 977, 1982.
 - [86] A. M. Cazabat, N. Fraysse, and F. Heslot. Thin wetting films. *Colloids and Surfaces*, 52:1 – 8, 1991.
 - [87] F. Heslot, A. M. Cazabat, P. Levinson, and N. Fraysse. Experiments on wetting on the scale of nanometers: Influence of the surface energy. *Phys. Rev. Lett.*, 65:599 – 602, 1990.
 - [88] S. Bardon, M. Cachile, A. M. Cazabat, X. Fanton, M. P. Valignat, and S. Villette. Structure and dynamics of liquid films on solid surfaces. *Faraday Discuss.*, 104:307 – 316, 1996.
 - [89] M. P. Valignat, M. Voué, G. Oshanin, and A. M. Cazabat. Structure and dynamics of thin liquid films on solid substrates. *Colloids and Surfaces*, 154:25 – 31, 1999.
 - [90] J. Daillant, G. Zalczer, and J. J. Benattar. Spreading of smectic-A droplets: Structure and dynamics of terraces. *Phys. Rev. A*, 46:6158 – 6162, 1992.
 - [91] S. Bardon, R. Ober, M. P. Valignat, F. Vandenbrouck, A. M. Cazabat, and J. Daillant. Organization of cyanobiphenyl liquid crystal molecules in prewetting films spreading on silicon wafers. *Phys. Rev. E*, 59:6808 – 6818, 1999.
 - [92] S. Betelú, B. Law, and C. C. Huang. Spreading dynamics of terraced droplets. *Phys. Rev. E*, 59:6699 – 6707, 1999.
 - [93] X. Ma, J. Gui, L. Smoliar, K. Grannen, B. Marchon, C. L. Bauer, and M. S. Jhon. Complex

- terraced spreading of perfluoropolyalkylether films on carbon surfaces. *Phys. Rev. E*, 59:722 – 727, 1999.
- [94] R. Lucht and Ch. Bahr. Surface plasmon resonance study of the spreading of a liquid-crystal smectic-A droplet on a gold substrate. *Phys. Rev. Lett.*, 85:4080 – 4084, 2000.
- [95] O. Ou Ramdane, P. Auroy, and P. Silberzan. Wetting of polymer brushes by a nematogenic compound. *Phys. Rev. Lett.*, 80:5141 – 5144, 1998.
- [96] P. Lazar, H. Schollmeyer, and H. Riegler. Spreading and two-dimensional mobility of long-chain alkanes at solid/gas interfaces. *Phys. Rev. Lett.*, 94:116101, 2005.
- [97] L. Xu, M. Salmeron, and S. Bardon. Wetting and molecular orientation of 8CB on a silicon substrate. *Phys. Rev. Lett.*, 84:1519 – 1522, 2000.
- [98] M. Voué, M. P. Valignat, G. Oshanin, A. M. Cazabat, and J. De Coninck. Dynamics of spreading of liquid microdroplets on substrates of increasing surface energies. *Langmuir*, 14:5951 – 5958, 1998.
- [99] U. Albrecht, A. Otto, and P. Leiderer. Two-dimensional liquid polymer diffusion: experiment and simulations. *Phys. Rev. Lett.*, 68:3192 – 3195, 1992.
- [100] V. J. Novotny. Migration of liquid polymers on solid surfaces. *J. Chem. Phys.*, 92:3189 – 3196, 1990.
- [101] N. Fraysse, M. P. Valignat, A. M. Cazabat, F. Heslot, and P. Levinson. The spreading of layered microdroplets. *J. Colloid Interface Sci.*, 158:27 – 32, 1993.
- [102] T. M. O'Connor, M. S. Jhon, C. L. Bauer, B. G. Min, D. Y. Yoon, and T. E. Karis. Surface diffusion and flow activation energies of perfluoropolyalkylether. *Tribol. Lett.*, 1:219 – 223, 1995.
- [103] T. M. O'Connor, Y. R. Back, M. S. Jhon, B. G. Min, and T. E. Karis. Surface diffusion of thin perfluoropolyalkylether films. *J. Appl. Phys.*, 79:5788 – 5790, 1996.
- [104] B. G. Min, J. W. Choi, H. R. Brown, D. Y. Yoon, T. M. O'Connor, and M. S. Jhon. Spreading characteristics of thin liquid films of perfluoropolyalkylethers on solid surfaces. Effects of chain-end functionality and humidity. *Tribol. Lett.*, 1:225 – 232, 1995.
- [105] M. P. Valignat, G. Oshanin, S. Villette, A.-M. Cazabat, and M. Moreau. Molecular weight dependence of spreading rates of ultrathin polymeric films. *Phys. Rev. Lett.*, 80:5377 – 5380, 1998.
- [106] M. Voué, M. P. Valignat, G. Oshanin, and A. M. Cazabat. Dissipation processes at the mesoscopic and molecular scale. The case of polymer films. *Langmuir*, 15:1522 – 1527, 1999.
- [107] S. Villette, M. P. Valignat, A. M. Cazabat, L. Jullien, and F. Tiberg. Wetting on the molecular scale and the role of water. A case study of wetting of hydrophilic silica surfaces. *Langmuir*, 12:825 – 830, 1996.
- [108] E. Pérez, E. Schäffer, and U. Steiner. Spreading dynamics of polydimethylsiloxane drops: crossover from Laplace to van der Waals spreading. *J. Colloid Interf. Sci.*, 234:178 – 193, 2001.
- [109] H. P. Kavehpour, B. Ovrin, and G. H. McKinley. Microscopic and macroscopic structure of the precursor layer in spreading viscous drops. *Phys. Rev. Lett.*, 91:196104, 2003.
- [110] F. Tiberg and A. M. Cazabat. Self-assembly and spreading of non-ionic trisiloxane surfactants. *Europhys. Lett.*, 25:205 – 210, 1994.
- [111] F. Tiberg and A. M. Cazabat. Spreading of thin films of ordered non-ionic surfactants. Origin of the stepped shape of the spreading precursor. *Langmuir*, 10:2301 – 2306, 1994.
- [112] G. Prévot, C. Cohen, J.-M. Guigner, and D. Schmaus. Macroscopic and mesoscopic surface diffusion from a deposit formed by a Stranski-Krastanov type of growth: Pb on Cu(100) at above one layer of coverage. *Phys. Rev. B*, 61:10393 – 10403, 2000.
- [113] K.H. Humfeld, S. Garoff, and P. Wynblatt. Analysis of pseudopartial and partial wetting of various substrates by lead. *Langmuir*, 20:2726 – 2729, 2004.
- [114] J. Moon, J. Lowekamp, P. Wynblatt, S. Garoff, and R. M. Suter. Effects of concentration dependent diffusivity on the growth of precursing films of Pb on Cu(111). *Surf. Sci.*, 488:73 – 82, 2001.
- [115] J. Moon, P. Wynblatt, S. Garoff, and R. Suter. Pseudopartial wetting and precursor film growth in immiscible metal systems. *Langmuir*, 20:402 – 408, 2004.
- [116] J. Moon, P. Wynblatt, S. Garoff, and R. Suter. Diffusion kinetics of Bi and Pb-Bi monolayer precursing films on Cu(111). *Surf. Sci.*, 559:149 – 157, 2004.
- [117] J. P. Monchoux, D. Chatain, and P. Wynblatt. On Auger microscopy study of the meeting and interdiffusion of pure Pb and Bi adsorbed layers on polycrystalline Cu. *Surf. Sci.*, 575:69 – 74, 2005.
- [118] J. P. Monchoux, D. Chatain, and P. Wynblatt. Impact of surface phase transitions and

- structure on surface diffusion profiles of Pb and Bi over Cu(100). *Surf. Sci.*, 600:1265 – 1276, 2006.
- [119] P. Wynblatt, D. Chatain, A. Ranguis, J. P. Monchoux, J. Moon, and S. Garoff. Factors affecting the coverage dependence of the diffusivity of one metal over the surface of another. *Int. J. of Thermophys.*, 28:646 – 660, 2007.
 - [120] D. Bonn, J. Meunier, and J. Indekeu. Comment on pseudopartial wetting and precursor film growth in immiscible metal systems. *Langmuir*, 21:3722 – 3723, 2005.
 - [121] C. Matano. On the relation between the diffusion-coefficients and concentrations of solid metals (the nickel - copper system). *Jpn. J. Phys.*, 8:109 – 113, 1933.
 - [122] P. G. de Gennes and A. M. Cazabat. Spreading of a stratified incompressible droplet. *C. R. Acad. Sci. Paris II*, 310:1601 – 1606, 1990.
 - [123] D. B. Abraham, P. Collet, J. De Coninck, and F. Dunlop. Langevin dynamics of spreading and wetting. *Phys. Rev. Lett.*, 65:195 – 198, 1990.
 - [124] D. B. Abraham, P. Collet, J. De Coninck, and F. Dunlop. Langevin dynamics of an interface near a wall. *J. Stat. Phys.*, 61:509 – 532, 1990.
 - [125] J. De Coninck, F. Dunlop, and F. Menu. Spreading of a solid-on-solid drop. *Phys. Rev. E*, 47:1820 – 1823, 1993.
 - [126] S. F. Burlatsky, G. Oshanin, A. M. Cazabat, and M. Moreau. Microscopic model of upward creep of an ultrathin wetting film. *Phys. Rev. Lett.*, 76:86 – 89, 1996.
 - [127] S. F. Burlatsky, G. Oshanin, A. M. Cazabat, M. Moreau, and W. P. Reinhardt. Spreading of a thin wetting film: microscopic approach. *Phys. Rev. E*, 54:3832 – 3845, 1996.
 - [128] S. F. Burlatsky, A. M. Cazabat, M. Moreau, G. Oshanin, and S. Villette. Spreading of molecularly thin wetting films on solid interfaces. In E. Tirapegui, J. Martinez, and R. Tiemann, editors, *Nonlinear Phenomena and Complex Systems*, Instabilities and Non-Equilibrium Structures VI, pages 233 – 267. Kluwer Academic Publishers, Dordrecht, 2000.
 - [129] G. Oshanin, J. De Coninck, A. M. Cazabat, and M. Moreau. Dewetting, partial wetting, and spreading of a two-dimensional monolayer on solid surface. *Phys. Rev. E*, 58:20 – 23, 1998.
 - [130] G. Oshanin, J. De Coninck, A. M. Cazabat, and M. Moreau. Microscopic model for spreading of a two-dimensional monolayer. *J. Mol. Liquids*, 76:195 – 219, 1998.
 - [131] M. N. Popescu and S. Dietrich. Model for spreading of liquid monolayers. *Phys. Rev. E*, 69:061602, 2004.
 - [132] A. Lukkarinen, K. Kaski, and D. B. Abraham. Mechanisms of fluid spreading: Ising model simulations. *Phys. Rev. E*, 51:2199 – 2202, 1995.
 - [133] D. B. Abraham, R. Cuerno, and M. Esteban. Microscopic model for thin film spreading. *Phys. Rev. Lett.*, 88:206101, 2002.
 - [134] K. Binder and D. W. Heermann. *Monte Carlo simulation in Statistical Physics: An Introduction*. Springer, Heidelberg, 2010.
 - [135] D. Frenkel and S. Berend. *Understanding molecular simulation: from algorithms to applications*. Academic Press, San Diego, 1996.
 - [136] D. B. Abraham, J. Heiniö, and K. Kaski. Computer simulation studies of fluid spreading. *J. Phys. A*, 24:L309 – L316, 1991.
 - [137] D. B. Abraham, P. Collet, J. De Coninck, F. Dunlop, J. Heiniö, K. Kaski, and L.-F. Ko. Theory of wetting and spreading. *Physica A*, 172:125 – 136, 1991.
 - [138] J. Heiniö, K. Kaski, and D. B. Abraham. Dynamics of a microscopic droplet on a solid surface: Theory and simulation. *Phys. Rev. B*, 45:4409 – 4416, 1992.
 - [139] A. Lukkarinen, K. Kaski, and D. B. Abraham. Mechanisms of fluid spreading: Ising model simulations. *Phys. Rev. E*, 51:2199 – 2202, 1995.
 - [140] J. De Coninck, S. Hoorelbeke, M. P. Valignat, and A.-M. Cazabat. Effective microscopic model for the dynamics of spreading. *Phys. Rev. E*, 48:4549 – 4555, 1993.
 - [141] J. De Coninck, N. Fraysse, M. P. Valignat, and A.-M. Cazabat. A microscopic simulation of the spreading of layered droplets. *Langmuir*, 9:1906 – 1909, 1993.
 - [142] A. M. Lacasta, J. M. Sancho, F. Sagues, and G. Oshanin. Propagation dynamics of a particle phase in a single-file pore. In J. M. Drake, J. Klafter, P. Levitz, R. M. Overney, and M. Urbakh, editors, *Mat. Res. Soc. Symp. Proc.*, volume 651, pages T9.1.1 – T9.1.12. Materials Research Society, Pittsburgh, PA, 2001.
 - [143] C. Dotti, A. Gambassi, M.N. Popescu, and S. Dietrich. Spreading in narrow channels. *Phys. Rev. E*, 76:041127, 2007.
 - [144] Milchev A. and Binder K. Droplet spreading: A Monte Carlo test of Tanner’s law. *J. Chem. Phys.*, 116:7691 – 7694, 2002.
 - [145] J. De Coninck. Spreading of chain-like liquid droplets on solids. *Colloids Surf. A*, 114:155 – 160, 1996.

- [146] M. Voué and J. De Coninck. Spreading and wetting at the microscopic scale: recent developments and perspectives. *Acta Mater.*, 48:4405 – 4417, 2000.
- [147] D. R. Heine, G. S. Grest, and E. B. Webb. Spreading dynamics of polymer nanodroplets. *Phys. Rev. E*, 68:061603, 2003.
- [148] V. M. Samsonov. On computer simulation of droplet spreading. *Curr. Opin. Colloid & Interface Sci.*, 16:303 – 309, 2011.
- [149] J.X. Yang, J. Koplik, and J. R. Banavar. Molecular dynamics of drop spreading on a solid surface. *Phys. Rev. Lett.*, 67:3539 – 3542, 1991.
- [150] J.X. Yang, J. Koplik, and J. R. Banavar. Terraced spreading of simple liquids on solid surfaces. *Phys. Rev. A*, 46:7738 – 7749, 1992.
- [151] J. A. Nieminen, D. B. Abraham, M. Karttunen, and K. Kaski. Molecular dynamics of a microscopic droplet on solid surface. *Phys. Rev. Lett.*, 69:124 – 127, 1992.
- [152] J. A. Nieminen and T. Ala-Nissila. Spreading dynamics of polymer microdroplets: A molecular-dynamics study. *Phys. Rev. E*, 49:4228 – 4236, 1994.
- [153] J. De Coninck, U. D’Ortona, J. Koplik, and J. R. Banavar. Terraced spreading of chain molecules via molecular dynamics. *Phys. Rev. Lett.*, 74:928 – 930, 1995.
- [154] U. D’Ortona, J. De Coninck, J. Koplik, and J. R. Banavar. Terraced spreading mechanisms for chain molecules. *Phys. Rev. E*, 53:562 – 569, 1996.
- [155] S. Bekink, S. Karaborni, G. Verbist, and K. Esselink. Simulating the spreading of a drop in the terraced wetting regime. *Phys. Rev. Lett.*, 76:3766 – 3769, 1996.
- [156] M. Haataja, J. A. Nieminen, and T. Ala-Nissila. Molecular ordering of precursor films during spreading of tiny liquid droplets. *Phys. Rev. E*, 52:R2165 – R2167, 1995.
- [157] M. Voué, S. Rovillard, J. De Coninck, M.P. Valignat, and A. M. Cazabat. Spreading of liquid mixtures at the microscopic scale: a Molecular Dynamics study of the surface-induced segregation process. *Langmuir*, 16:1428 – 1435, 2000.
- [158] D. R. Heine, G. S. Grest, and E. B. Webb. Spreading dynamics of polymer nanodroplets in cylindrical geometries. *Phys. Rev. E*, 70:011606, 2004.
- [159] E. B. Webb, G. S. Grest, and D. R. Heine. Precursor film controlled wetting of Pb on Cu. *Phys. Rev. Lett.*, 91:236102, 2003.
- [160] D. R. Heine, G. S. Grest, and E. B. Webb. Surface wetting of liquid nanodroplets: droplet-size effects. *Phys. Rev. Lett.*, 95:107801, 2005.
- [161] N. Sedihi, S. Murad, and S. K. Aggarwal. Molecular dynamics simulations of spontaneous spreading of a nanodroplet on solid surfaces. *Fluid Dyn. Res.*, 43:015507, 2011.
- [162] C. Wu, T. Qian, and P. Sheng. Droplet spreading driven by van der Waals force: a molecular dynamics study. *J. Phys.: Condens. Matter*, 22:325101, 2010.
- [163] J. Moon, J. Yoon, P. Wynblatt, S. Garoff, and R.M. Suter. Simulation of spreading of precursing Ag films on Ni(100). *Comp. Mat. Sci.*, 25:503 – 509, 2002.
- [164] E. B. Webb, G. S. Grest, D. R. Heine, and J. J. Hoyt. Dissolutive wetting of Ag on Cu: A molecular dynamics simulation study. *Acta Materialia*, 53:3163 – 3177, 2005.
- [165] Y. Sun and E. B. Webb. The atomistic mechanism of high temperature contact line advancement: results from molecular dynamics simulations. *J. Phys.: Condens. Matter*, 21:464135, 2009.
- [166] Q. Yuan and Y. P. Zhao. Precursor film in dynamic wetting, electrowetting, and electro-elasto-capillarity. *Phys. Rev. Lett.*, 104:246101, 2010.
- [167] T. Smith. The hydrophilic nature of a clean gold surface. *J. Colloid Interf. Sci.*, 75:51 – 55, 1980.
- [168] A. Hoang and H.P. Kavehpour. Dynamics of nanoscale precursor films near a moving contact line of spreading drops. *Phys. Rev. Lett.*, 106:254501, 2011.
- [169] H. Xu, D. Shirvanyants, K. Beers, K. Matyjaszewski, M. Rubinstein, and S. S. Sheiko. Molecular motion in a spreading precursor film. *Phys. Rev. Lett.*, 93:206103, 2004.
- [170] S. Villette, M. P. Valignat, A.-M. Cazabat, F. A. Schabert, and A. Kalachev. Ultrathin liquid films. Ellipsometric study and AFM preliminary investigations. *Physica A*, 263:123 – 129, 1997.
- [171] D. Glick, P. Thiansathaporn, and R. Superfine. In situ imaging of polymer melt spreading with a high-temperature atomic force microscope. *Appl. Phys. Lett.*, 71:206103, 1997.
- [172] Glynos. E., B. Frieberg, and P. F. Green. Wetting of a multiarm star-shaped molecule. *Phys. Rev. Lett.*, 107:118303, 2011.
- [173] S. S. Chibbaro, L. Biferale, F. Diotallevi, S. Succi, K. Binder, D. Dimitrov, A. Milchev, S. Girardo, and D. Pisignano. Evidence of thin-film precursors formation in hydrokinetic and atomistic simulations of nano-channel capillary filling. *EPL*, 84:44003, 2008.
- [174] S. Douezan, K. Guevorkian, R. Naouar, S. Dufour, D. Cuvelier, and F. Brochard-Wyart.

- Spreading dynamics and wetting transition of cellular aggregates. *Proc. Natl. Acad. Sci. USA*, 108:7315 – 7320, 2011.
- [175] S. Douezan, J. Dumond, and F. Borchard-Wyart. Wetting transitions of cellular aggregates induced by substrate rigidity. *Soft Matter*, 8:4578 – 4583, 2012.
 - [176] N. Pesheva and G. Oshanin. Monolayer spreading on a chemically heterogeneous substrate. *Colloids and Surfaces A*, 206:349 – 361, 2002.
 - [177] M. N. Popescu and S. Dietrich. Spreading of liquid monolayers: from kinetic Monte Carlo simulations to continuum limit. In H. Emmerich, B. Nestler, and M. Schreckenberg, editors, *Interface and transport dynamics: computational modelling*, pages 202 – 207. Springer, Berlin, 2003.
 - [178] O. Bliznyuk, H. P. Jansen, E. S. Kooij, H. J. W. Zandvliet, and B. Poelsema. Smart design of stripe-patterned gradient surfaces to control droplet motion. *Langmuir*, 27:11238 – 11245, 2011.
 - [179] A. Moosavi, M. Rauscher, and S. Dietrich. Motion of nanodroplets near edges and wedges. *Phys. Rev. Lett.*, 97:236101, 2006.
 - [180] A. Moosavi, M. Rauscher, and S. Dietrich. Motion of nanodroplets near chemical heterogeneities. *Langmuir*, 24:734 – 742, 2008.
 - [181] A. Moosavi, M. Rauscher, and S. Dietrich. Size dependent motion of nanodroplets on chemical steps. *J. Chem. Phys.*, 129:044706, 2008.
 - [182] M. Rauscher and S. Dietrich. Nano-droplets on structured substrates. *Soft Matter*, 5:2997 – 3001, 2009.
 - [183] A. Moosavi, M. Rauscher, and S. Dietrich. Dynamics of nanodroplets on topographically structured substrates. *J. Phys.: Condens. Matter*, 21:464120, 2009.
 - [184] M. N. Popescu, S. Dietrich, and G. Oshanin. Diffusive spreading and mixing of fluid monolayers. *J. Phys.: Condens. Matter*, 17:S4189 – S4198, 2005.
 - [185] C. Lv, C. Chen, Y.-C. Chuang, F.-G. Tseng, Y. Yin, F. Grey, and Q. Zheng. Driving droplets by curvi-propulsion. *arXiv:1202.6582v1*, 2012.
 - [186] Q.Z. Yuan and Y.P. Zhao. Topology-dominated dynamic wetting of the precursor chain in a hydrophilic interior corner. *Proc. Roy. Soc. A*, 468:310 – 322, 2012.
 - [187] K. L. Maki and S. Kumar. Fast evaporation of spreading droplets of colloidal suspensions. *Langmuir*, 27:11347 – 11363, 2011.